

ELUCIDATION OF CHEMICAL PROCESSES IN COAL LIQUEFACTION: EFFECT OF RADICAL QUENCHERS

Tetsuo Aida, Bogdan Slomka, and Thomas G. Squires*

Ames Laboratory
Iowa State University
Ames, Iowa 50011

INTRODUCTION

The thermal liquefaction of coal is a complex, heterogeneous process involving two mutually interactive phenomena: chemical transformation of the organic material and mass transfer between solid, liquid, and gaseous phases (1,2). Thermally generated free radicals play a key role in these conversions; and their subsequent interactions with other species, e.g. hydrogen donors, determine the course of the liquefaction process and the final product mixture (3,4). In functional terms, the organic portion of coal can be described as a two component system: a cross-linked macromolecular network constituting an insoluble, immobile phase; and a low molecular weight, soluble bitumen component comprising a mobile phase (5,6).

Since bitumen is already a soluble low molecular weight material, it should not be considered a liquefaction target. The liquefaction objective is chemical unlinking of the macromolecular coal network. From this perspective, it is important to obtain experimental information about the behavior of the insoluble macromolecular portion of coal during liquefaction. Conventional batch mode experimental techniques which confine starting materials, intermediates, and products to the same reaction space throughout the entire course of conversion cannot provide this information.

Bitumen is reactive under liquefaction conditions (7); and its hydrogen donor/shuttler ability is well established (8,9). Thermal chemical reactions involving bitumen are thus apt to obscure the primary liquefaction processes, i.e. disruption of the macromolecular network. In order to isolate the thermal chemical behavior of the macromolecular component, we have sought to minimize contributions due to bitumen by using pyridine extracted coal. To avoid similar screening effects arising from the lingering presence of liquefaction products, we have developed a short residence time, flow mode micro-reactor which rapidly removes solubilized material from the reaction zone. Using this approach, the response of the insoluble coal matrix to various chemical reagents can be evaluated with minimal interference from bitumen or liquefaction products. In the present study, we have investigated the effects of radical quenchers, radical initiators, and chain transfer agents on the thermal solubilization of pyridine extracted Illinois No.6 coal in benzene.

* Present address: Associated Western Universities, Inc., 142 East
200 South, Suite 200, Salt Lake City, UT 84111.

EXPERIMENTAL

General

Illinois No. 6 coal from the Ames Laboratory Coal Library was used in these studies. Prior to use, the coal was ground and sized to 100-200 mesh under a nitrogen atmosphere and dried overnight at 110 C under vacuum. The ultimate analysis for this coal (dmmf basis) is C : 80.6%; H : 5.6%; N : 1.6%; S : 2.4%; O(diff): 9.8%. Ash (dry basis) and volatile matter (daf basis) contents are 10.0% and 40.4%, respectively. For these solubilization experiments, coal was Soxhlet extracted with pyridine under nitrogen for two days; and the residue was dried overnight at 110C under vacuum. Solvents, solutions of reagents, and effluent samples were handled and stored under nitrogen. HPLC grade solvents were degassed by sonication, distilled under nitrogen, and introduced directly into the reactor system. Chemical reagents were used as received from commercial sources.

Solubilization Procedures

Solubilization experiments were carried out in a 300 μ L rapid heating, flow mode tubular microreactor. The construction and general configuration of the apparatus and reactor unit have been described previously (10). Important features of the reactor system include temperature and pressure programming capability, continuous, "on-line" optical density monitoring of the reactor effluent; real time acquisition of optical density, temperature, and pressure data; and a time resolved product collection system.

In a typical experiment, approximately 200 mg of 100-200 mesh pre-extracted coal was placed in the reactor, fixed in place by 2M stainless steel frits, and a shielded 0.062 inch o.d. chromel-alumel thermocouple was inserted into the coal bed. After connecting the reactor and purging with nitrogen, the reactor was pressurized, filled with benzene or a solution of reagent in benzene, and the flow rate was adjusted to 1.0 mL/minute. Tetrahydrofuran (THF) was then introduced into the reactor effluent immediately after the exit at a flow rate of 1.0 mL/minute. The system was maintained at a constant pressure of 3000 psi throughout the experiment; and, under these conditions, the residence time of the fluid in the reactor was approximately 5 seconds. The temperature profile of the coal bed was controlled from 20 C to 430 C according to a predetermined program.

Typically, ten aliquots were collected from the reactor during a 70 minute experiment. At the end of the experiment, the reactor was quickly cooled to room temperature while purging with nitrogen; and the residue was removed from the reactor and weighed. The reactor effluent was analyzed with a Varian 3700 Gas Chromatograph equipped with a 30 meter OV-101 fused silica capillary column using internal standards for quantitation.

RESULTS AND DISCUSSION

Overall conversions of coal in the thermal solubilization experiments were determined gravimetrically. Conversions were found to be positive or negative depending, presumably, on the balance between loss of solubilized fragments and uptake of reactive species supplied to the reaction zone reagent solutions. Monitoring of the optical density of the solubilization products gave us further insight into the dynamics of the thermal behavior of coal during solubilization. While it is clear that the latter technique mixes qualitative effects (different species) with quantitative ones

(concentrations), we have found the Integrated Absorbance (IA) to correlate significantly with the gravimetrically determined conversions in several solvents (10). Integrated Absorbance thus provides a useful approximation of yields and rates of coal conversions in these systems.

Figure 1 shows an excellent linear regression fit for IA vs Weight Loss for Illinois No. 6 coal. Data for this plot were taken from thermal solubilization experiments at different temperatures and pressures using benzene as the solvent. We have used such optical density profiles to reveal and investigate differences in solubilization rates for coals of different rank (10), and as the basis for collecting effluent fractions during solubilization (11).

Figure 2 depicts typical kinetograms obtained by this method for raw and pyridine pre-extracted Illinois No. 6 coal. It is clear that the first peak in the raw coal profile is due to pyridine soluble material (i.e. bitumen), eluted between 130 and 320°C. In the benzene solubilization of Illinois No. 6 coal, we have previously established that below 300°C the effluent is comprised, almost exclusively, of physically extracted components, while at higher temperatures thermal processes predominate (12). Thus the kinetogram of pyridine extracted coal reasonably represents the thermal chemical behavior of the macromolecular portion of coal. Gravimetric conversions (dry basis) for the raw coal and the extracted coal are 51.6% and 31.8%, respectively; it is interesting to note that the corresponding ratios of the conversions and the integrated absorbances are 1.62 and 1.58.

Effect of Hydrogen Donors

Thermal liquefaction of coal is generally considered to proceed via radical processes initiated by homolytic cleavages of weak covalent bonds, e.g. bibenzyl or benzyl ether linkages (13). From a radical chemistry perspective, the hydrogen donors commonly used in coal liquefaction are simply radical quenchers (14). Therefore, the thermal solubilization behavior of the pyridine pre-extracted coal in the presence of hydrogen donors will provide useful information about radical processes occurring in the coal matrix during thermal liquefaction. **Figure 3** shows the Thermal Solubilization Profile (TSP) of pyridine pre-extracted Illinois No. 6 coal generated in the presence of 5.0 mole percent THN solution compared with the TSP of pure benzene. The gravimetric conversions (dry basis) were 46.4% and 31.8%, respectively.

Comparison of the two curves reveals a relative increase in the optical density of the THN experiment commencing at about 330°C; this is a clear indication of the onset of radical processes. More detailed information about the effects of THN can be gleaned from a plot of the ratio of the absorbances vs temperature, also shown in **Figure 3**. The effectiveness of THN gradually increased between 330 and 400°C followed by a sharp increase in the ratio. The latter increase is coincident with the significant decline in the TSP of the reference run. This probably indicates the onset of retrogressive process, e.g. char formation, in the absence of a hydrogen donor. Furthermore, the distinct inflection of the ratio curve suggests that there are two levels of reactivity in the coal matrix.

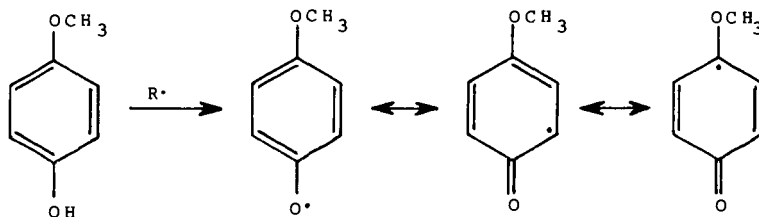
The relative effects of 9,10-dihydroanthracene (DHA) and tetralin on the Thermal Solubilization Profiles of pre-extracted Illinois No. 6 coal are compared in **Figure 4**. In these experiments, 1.0 mole percent solutions of DHA and THN in benzene were used. The TSP generated with pure benzene is provided for comparison. The respective gravimetric conversions for DHA, THN, and benzene are 71.5%; 35.5% and 32.7%. Based on these data, DHA is about 12 times

more efficient than THN. Kamiya, et al. compared the reactivities of these two hydrogen donors in batch mode liquefaction of a Japanese bituminous coal and concluded that DHA is 12.5 to 14.5 times more reactive than THN (15). This close agreement with our results indicates that the reactivities of bitumen, primary liquefaction products, and the macromolecular matrix of coal are all very similar with respect to hydrogen abstraction from hydrogen donors.

Additional information about the thermal behavior of pre-extracted coal can be drawn from the concentration profiles of DHA and anthracene (AN) also shown in Figure 4. The molar concentrations of these species in the reactor effluent were analyzed by GC and corrected for the decomposition of DHA (ca. 6% at 430 C). There is a qualitative similarity between the Thermal Solubilization Profile and the DHA and AN concentration profiles; and this provides additional confirmation that thermal chemical unlinking of the coal matrix is controlled by radical processes. Although it is not clear how accurately these concentration profiles mirror rates of primary liquefaction processes, the slowly decaying AN concentration at later stages of the solubilization (40-70 minutes, 420-430°C) strongly suggests that there is still significant radical activity in the residual matrix.

Effect of the Radical Quencher

In order to further examine the role of the radical processes in the thermal chemical unlinking of pyridine pre-extracted Illinois No.6 coal, a 1 mole percent solution of p-methoxyphenol (PMP) was used to investigate the effects of radical quenchers. PMP is a powerful radical quencher, transconverting reactive radicals to a less reactive resonance stabilized one (16):



The experimental results are shown in Figure 5. The thermal stability of PMP itself was examined in a blank experiment with only a negligible loss of PMP. As in the case of the hydrogen donors, there was significant positive displacement of the Thermal Solubilization Profile compared to the benzene profile. However, the weight loss was only 27.5% compared to 32.7% for the benzene reference experiment; and it appears that PMP may have been incorporated into the coal matrix. This is consistent with the PMP concentration profile also shown in Figure 5. The incorporation appears to be at least partially reversible, with capture occurring in the first 30 minutes and release during the final 30 minutes.

Effect of the Radical Initiator

Diphenyldisulfide (DPDS) was used to investigate the effects of radical initiators on the thermal liquefaction of pyridine pre-extracted coal. The sulfur-sulfur bond in DPDS is known to cleave homolytically at 300°C (17); and, moreover, it is an effective chain

transfer reagent (18). Results of this experiment are summarized in **Figure 6**. From the Thermal Solubilization Profiles it seems clear that DPDS inhibits productive pathways, i.e. formation of soluble products, in the thermal chemical unlinking of the coal matrix. DPDS is converted in a large proportion to benzenethiol as shown in the concentration profiles in **Figure 6**. The only available source of hydrogen, which is necessary for the formation of BT, is coal. Thus, it appears that the primary effect of this radical initiator is hydrogen abstraction from the coal matrix. In addition, the gravimetric results show an 11.1% weight gain indicating trapping of reactive fragments by the coal matrix.

These results are in distinct contrast to those of Stock, et. al. (18). These workers observed substantial acceleration of the thermal dissolution of Illinois No.6 coal by diphenyl disulfide. However, their reactions were conducted in the batch mode on unextracted coal in the presence of excess tetralin so there are several possible explanations. Research is underway to assess the differences in the two systems.

ACKNOWLEDGEMENT

We wish to thank Professors R. S. Hansen and T. J. Barton for useful discussions and encouragement. We are also grateful for support from the State of Iowa and from the U.S. Department of Energy through the Ames Laboratory under Contract No. W-7405-ENG-86.

REFERENCES

1. Whitehurst, D.D.; Mitchell, T.O.; Farcasiu, M. "Coal Liquefaction: The Chemistry and Technology of Thermal Processes", Academic Press, New York, 1980.
2. Neuworth, M.B.; Gray, D. "Fundamental Aspects of Primary Coal Liquefaction", Contract No.58-0336, MITRE Report No. WP-85W00097, August, 1985.
3. Sprecher, R.F.; Retcofsky, H.L. Fuel 1983, 62, 473.
4. Stenberg, V.I.; Jones, M.B.; Suwarnasarn, N.J. Fuel 1985, 64, 470.
5. Marzec, A.; Jurkiewicz, A.; Pislewski, N. Fuel 1983, 62, 966.
6. Ref 2, pp 51-114.
7. Whitehurst, D.D.; Farcasiu, M.; Mitchell, T.O. "The Nature and Origin of Asphaltenes in Processed Coals" EPRI Report AF-480, July, 1977.
8. Neavel, R.C. Fuel 1976, 55, 237.
9. Whitehurst, D.D.; Mitchell, T.O. "Liquid Fuels from Coal", Ellington, R.T., ed., Academic Press, New York, 1977, p 153 ff.
10. Aida, T.; Slomka, B.; Shei, J.C.; Chen, Y.-Y.; Squires, T. G. Prepr. Pap.-Am. Chem. Soc., Div. Fuel Chem. 1985, 30 (4), 274.

11. Slomka, B.; Aida, T.; Chen, Y.-Y.; Junk, G.A.; Squires, T. G. Prepr. Pap.-Am. Chem. Soc., Div. Fuel Chem. **1986**, 31 (1), 238.
12. Squires, T.G.; Aida, T.; Chen, Y.-Y.; Smith, B.F. Prepr. Pap.-Am. Chem. Soc., Div. Fuel Chem. **1983**, 28 (4), 228.
13. Pullen, J.R. "Solvent Extraction of Coal", IEA Coal Research Report No. ICTIS/TR16, London, **1981**, p 35 ff.
14. Kim, S.S.; Jarand, M.L.; Durai-Swamy, K. Fuel **1984**, 63, 510.
15. Kamiya, Y.; Nagai, S.; Yao, T. "Relative Effectiveness of Aromatic Solvents in the Liquefaction of Brown Coal and Bituminous Coal", Proceedings, International Conference on Coal Science, Pittsburgh, August **1983**, 104.
16. Baker, C.W.; Shields, D.J. J. Polymer Sci. **1960**, 47, 498.
17. Field, L., Chap. 7 in "Organic Chemistry of Sulfur", Oae, S., ed., Plenum Press, New York, **1977**.
18. Stock, L.M.; Duran, J.E.; Huang, C.B.; Srinivas, V.R.; Willis, R. S. Fuel **1985**, 64, 754.

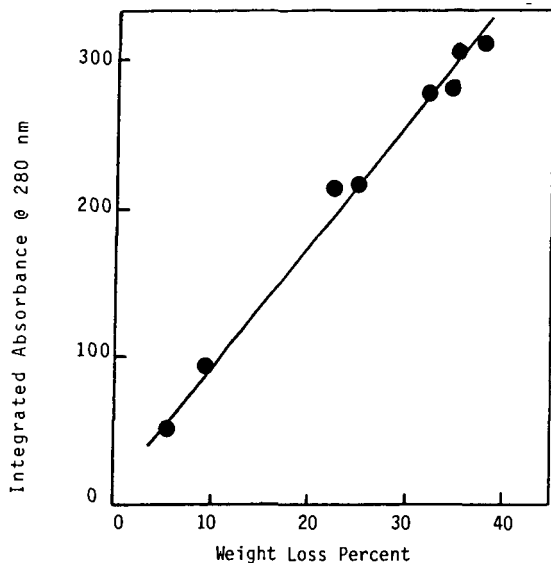


Figure 1. Correlation of Integrated Absorbance with Weight Loss in the Benzene Solubilization of Illinois No.6 Coal.

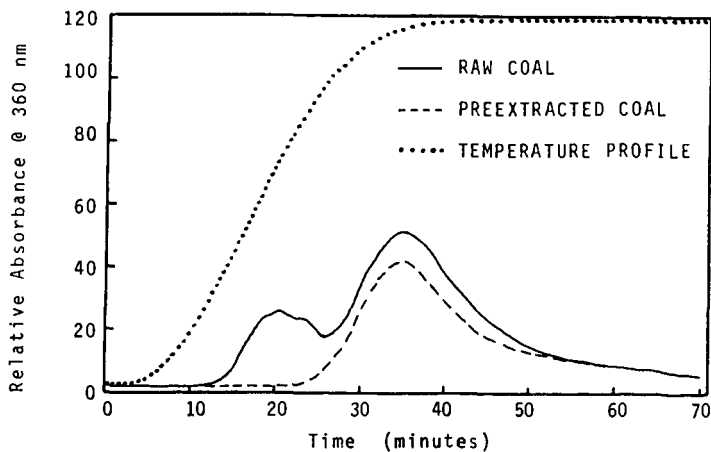


Figure 2. Temperature Programmed Benzene Solubilization Profiles of the Illinois No.6 Coal.

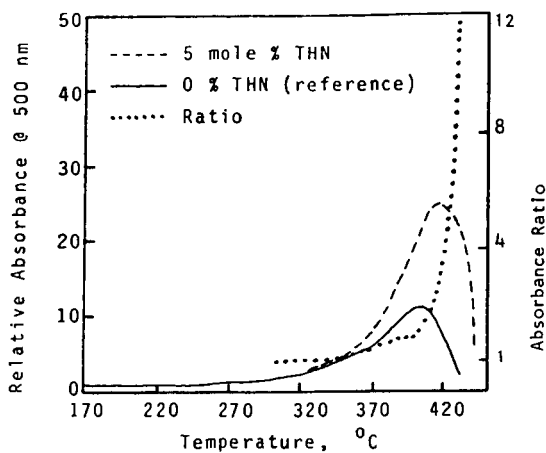


Figure 3. Effect of Tetralin (THN) on the Benzene Solubilization Profile of Pyridine Pre-extracted Illinois No.6 Coal.

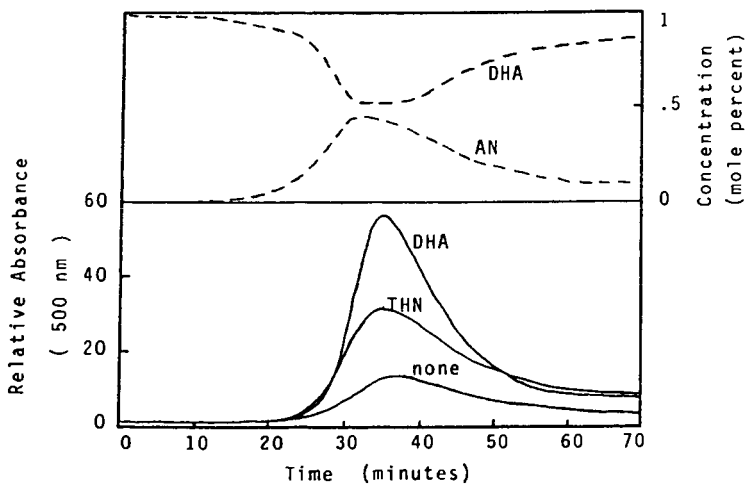


Figure 4. Hydrogen Donor Effects on the Benzene Solubilization Profile of the Pyridine Pre-extracted Illinois No.6 Coal. Top: 9, 10-Dihydroanthracene (DHA) and Anthracene (AN) Effluent Concentration Profiles. Bottom: Thermal Solubilization Profiles.

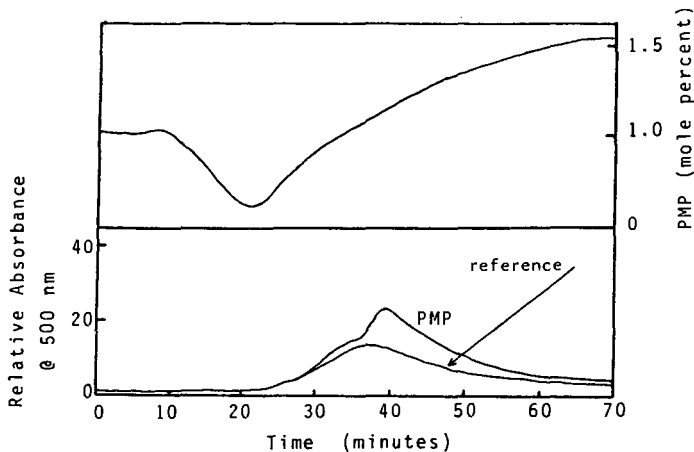


Figure 5. The Radical Scavenger Effect on the Thermal Solubilization Profiles of Pyridine Pre-extracted Illinois No.6 Coal. Top: Para-Methoxyphenol (PMP) Concentration Profile of Effluent. Bottom: PMP Effect on the Thermal Solubilization Profile.

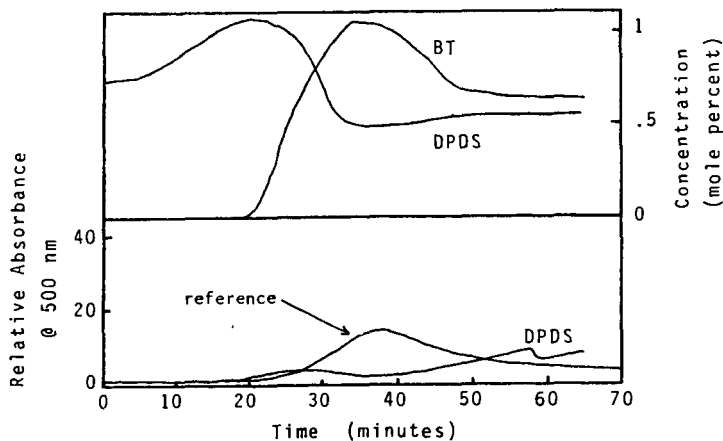


Figure 6. Radical Initiator Effect on the Thermal Solubilization of Pyridine Pre-extracted Illinois No.6 Coal. Top: Diphenyldisulfide (DPDS) and Benzenethiol (BT) Effluent Concentration Profiles. Bottom: DPDS Effect on the Thermal Solubilization Profile.

CATALYZED COAL CONVERSION USING WATER OR ALCOHOLS

Bradley C. Bockrath and Henry M. Davis

U.S. Department of Energy
Pittsburgh Energy Technology Center
P.O. Box 10940
Pittsburgh, Pennsylvania 15236

Water and some alcohols such as 1-octanol have certain properties that can be used to good advantage in coal liquefaction. The use of water as a liquefaction solvent has been explored in work reported earlier from this center.^{1,2} High conversions of coal were observed when water was used near or above its critical temperature in the presence of a good catalyst and molecular hydrogen.

Certain properties of water near its critical conditions are advantageous in relation to its use as a liquefaction solvent. Some of these have been discussed in a recent review³ and reports.^{4,5} Water near its critical conditions is an excellent solvent for many organic compounds. Liquefaction experiments that used water as a reaction medium and as a means to transport product oils from insoluble coal residues demonstrate clearly that liquefaction products from coal are soluble in water near the critical temperature and somewhat below the critical density.⁵ In addition, it has been reported that water may directly participate in the thermolytic chemistry of many model compounds, a few examples being quinoline,⁷ dibenzylether,⁸ and benzylphenol.⁹ Thus, it seems possible that water might act as both a physical solvent and a reactant when used as a liquefaction solvent.

Other experiments indicate that yields of tetrahydrofuran extracts determined after heating with water in the absence of hydrogen are a strong function of water density and are markedly lower at subcritical densities.⁶

The chemistry of this intriguing system was explored further by making a series of comparisons between water and a number of other solvents with critical temperatures near that of water. The solvents were chosen to cover a range of solvent power and functionality. Alcohols such as 1-octanol and 1,5-pentandiol gave conversions as high as those with water but at markedly lower total pressure.

EXPERIMENTAL

Detailed experimental procedures have been given.¹ In brief, a set of five 42-mL microautoclaves was used. The entire set was immersed into a preheated, fluidized sandbath. Cooling was provided by immersion in a second fluidized sandbath held at room temperature. Thus, five samples were subjected to nearly identical thermal profiles in one experiment. Agitation was provided by a pneumatic shaker to promote mixing.

The coal was an Illinois No. 6 (River King Mine) bituminous coal. The elemental analysis was C, 73.7%; H, 5.6%; N, 1.5%; O, 14.8%; and S, 4.5%, on a daf basis. The moisture-free ash content was 13.6%. Liquefaction solvents other than water were reagent-grade chemicals used without further purification. Ammonium paramolybdate was added either directly as a dry powder or as an aqueous solution to make 1000 ppm Mo on daf coal. Coal charge was 4.0 g (3.4 g daf) unless otherwise noted. A pressure of 1200 psig hydrogen was applied in all cases before heating. The liquefaction temperature was always 385°C. The critical temperature of water is 374.2°C.

The liquefaction products were recovered using tetrahydrofuran (THF) after pressure letdown. Conversions were determined using room-temperature extraction with

THF. Soluble portions were decanted from residues after centrifugation. Extractions were continued until the supernatant was nearly colorless. Conversion values were based on dry THF-insoluble residue. The reproducibility was usually within $\pm 2\%$.

RESULTS AND DISCUSSION

Previous work has shown that conversions obtained under hydrogen pressure in the presence of water are substantially higher than in its absence.¹ An increase in conversion was found both with and without added catalyst. The effectiveness of water must certainly rest in part on its ability to function as a physical solvent. Density is a key variable governing the solvent strength of water above the critical temperature. To probe the effect of water density on coal conversion, three sets of experiments were carried out. In one, the loading of coal was held constant, and the amount of added water was varied. Conversions measured as a function of time are shown in Figure 1. A second set of experiments was carried out with the ratio of water to coal held constant, but the total amount of both was varied (Figure 2). Finally, the water density was held constant, but the mass of coal was varied (Figure 3).

As may be seen, coal conversion approaches a plateau after reaction for 60 min at 385°C. Conversion is a strong function of water density over the range studied here. The maximum density used, 0.09 g/mL, is considerably below the density at the critical point, 0.315 g/mL. The density used in these experiments was limited by consideration of the total pressure in the autoclave at temperature. At the highest density, the total pressure was estimated to be 5300 psi, with 2600 psi due to hydrogen and 2700 psi due to water.

In the first set of experiments, both the water density and the relative amount of water to coal was varied. The data from the second set of experiments shown in Figure 2 indicate that the spread of conversion values as a function of water density is smaller if the water-to-coal ratio is held constant at 0.85. Nonetheless, water density remains an important determinant of coal conversion even when the relative amount of coal loading is removed as a variable.

Finally, if the amount of coal is increased while the water density is held constant at 0.09 g/mL, the conversion is decreased (Figure 3). Thus, taking the data together, both the water density and the relative amount of coal charged are important determinants of conversion. Conversion is favored by increasing water density and disfavored by increasing coal loading. Increasing density would improve the ability of water to dissolve coal conversion products. Increasing coal loading would increase the probability of retrogressive recombination reactions. The observed trends in conversion can be rationalized on the basis of the relative rate of retrogressive reactions, lower rates being favored by higher water densities and lower coal loadings.

Comparison was made between water and 1,2,4-trimethylbenzene (critical temperature = 378°C est.) to reveal whether it held unusual properties for liquefaction. In this comparison, conversions were measured after heating for 30 minutes at 385°C over the entire composition range of the binary mixtures from pure trimethylbenzene to pure water. The density of total amount of added solvents was always 0.09 g/mL.

The data contained in Figure 4 indicate that water is far superior to trimethylbenzene. In view of the success of toluene as a supercritical solvent for coal,¹⁰ trimethylbenzene might be expected to be a reasonably good liquefaction medium. The performance of water is all the more surprising by comparison.

Water contains hydroxyl groups that trimethylbenzene does not. Figure 4 also includes results obtained with two other hydroxyl-containing compounds, 1-octanol

(critical temperature = 385.5°C) and 1,5-pentanediol (critical temperature = 410°C est.). In binary mixtures with trimethylbenzene, these two alcohols are roughly as, or possibly more, effective than water. However, the alcohols would exert far less pressure than water at the same temperature.

The same data shown in Figure 4 are replotted in Figure 5 on the basis of the molar density of hydroxyl groups, that is, the mols of hydroxyl groups per liter of reactor space. The conversion values increase with hydroxyl density at markedly different rates. Thus, conversion does not depend simply on the total density of hydroxyl groups. This observation favors an interpretation on the basis of bulk solvent and/or diffusional effects rather than direct chemical participation of the hydroxyl group. However, further work is necessary to fully dissect the chemistry.

This preliminary work has shown that certain alcohols and water are effective liquefaction media at 385°C, a temperature near their critical temperatures. Solvency or diffusional effects seem to be the important variables governing conversion, although chemical effects cannot be entirely ruled out. The higher boiling alcohols, 1-octanol and 1,5-pentanediol, are as effective as water, yet their partial pressure for a given density is far lower than that of water.

REFERENCES

1. B.D. Blaustein, B.C. Bockrath, H.M. Davis, S. Friedman, E.G. Illig, and M.A. Mikita, Am. Chem. Soc. Div. Fuel Preprints, 30(2), 359-367 (1985).
2. J.A. Ruether, S. Friedman, E.G. Illig, and B.C. Bockrath, Proceedings, 1985 Int. Conf. Coal Science, 51-54, Pergamon Press, Sydney (1985).
3. D.S. Ross, "Coal Conversion in Carbon Monoxide-Water Systems" in Coal Science, Vol. 3, M.L. Gorbaty, J.W. Larsen, and I. Wender, Eds., Academic Press, New York, 301-338 (1984).
4. V.I. Stenberg, R.D. Hei, P.G. Sweeny, and J. Nowak, Am. Chem. Soc. Div. Fuel Preprints, 29(5), 63-66 (1984).
5. P. Barton, Ind. Eng. Chem., Process Des. Dev., 22, 589-594 (1983).
6. G.V. Deshpande, G.D. Holder, A.A. Bishop, J. Gopal, and I. Wender, Fuel, 63, 956-960 (1984).
7. T.J. Houser, D.M. Tiffany, Z. Li, M.E. McCarville, and M.E. Houghton, Fuel, 65, 827-832 (1986).
8. M.E. Paulaitis, M.T. Klein, and A.B. Stilles, DOE Quarterly Report, DE-FE22-82PC50799, July-Sept. (1983).
9. M.A. Mikita and H.T. Fish, Am. Chem. Soc. Div. Fuel Chem., 31(4), 56-63 (1986).
10. K.D. Bartle, T.G. Martin, and D.F. Williams, Fuel, 54, 226-235 (1975).

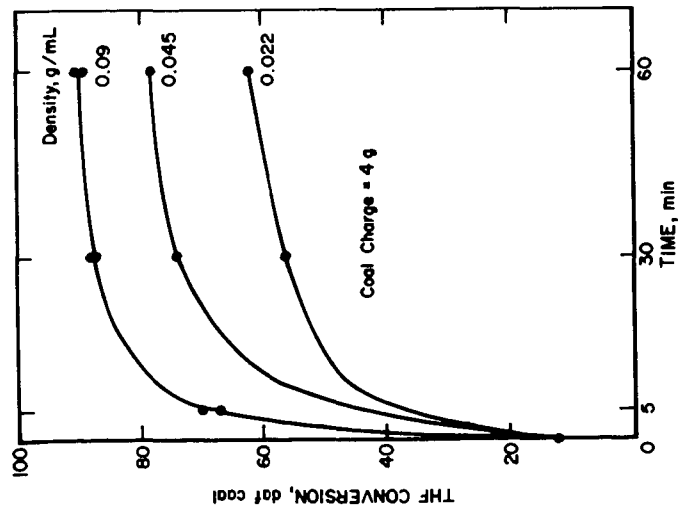


Fig. 1. Conversion and Water Density.

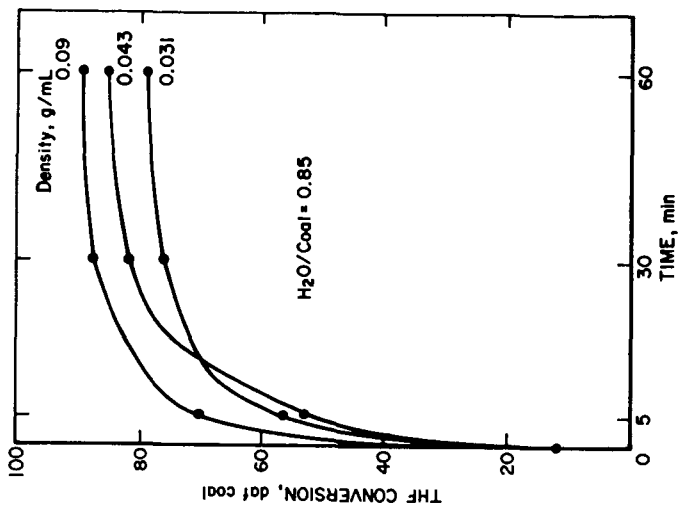


Fig. 2. Conversion and Water Density.

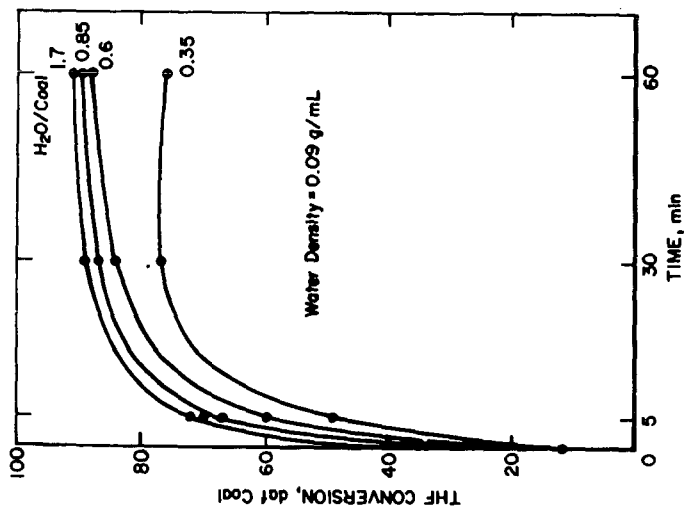


Fig. 3. Conversion and Coal Charge.

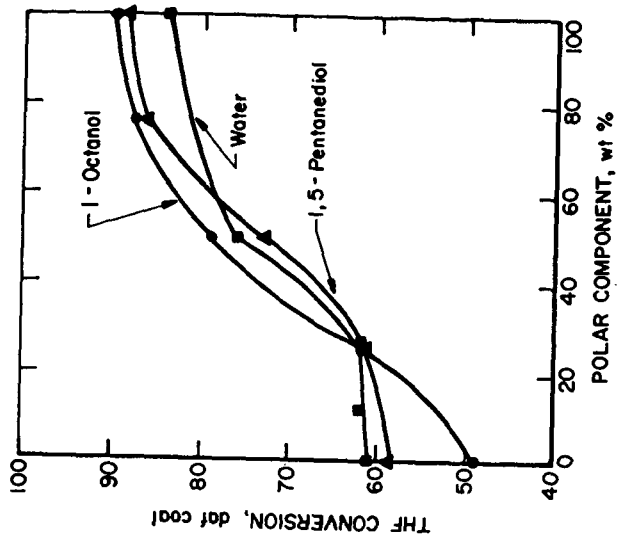


Fig. 4. Conversion in 1,2,4-Trimethylbenzene.

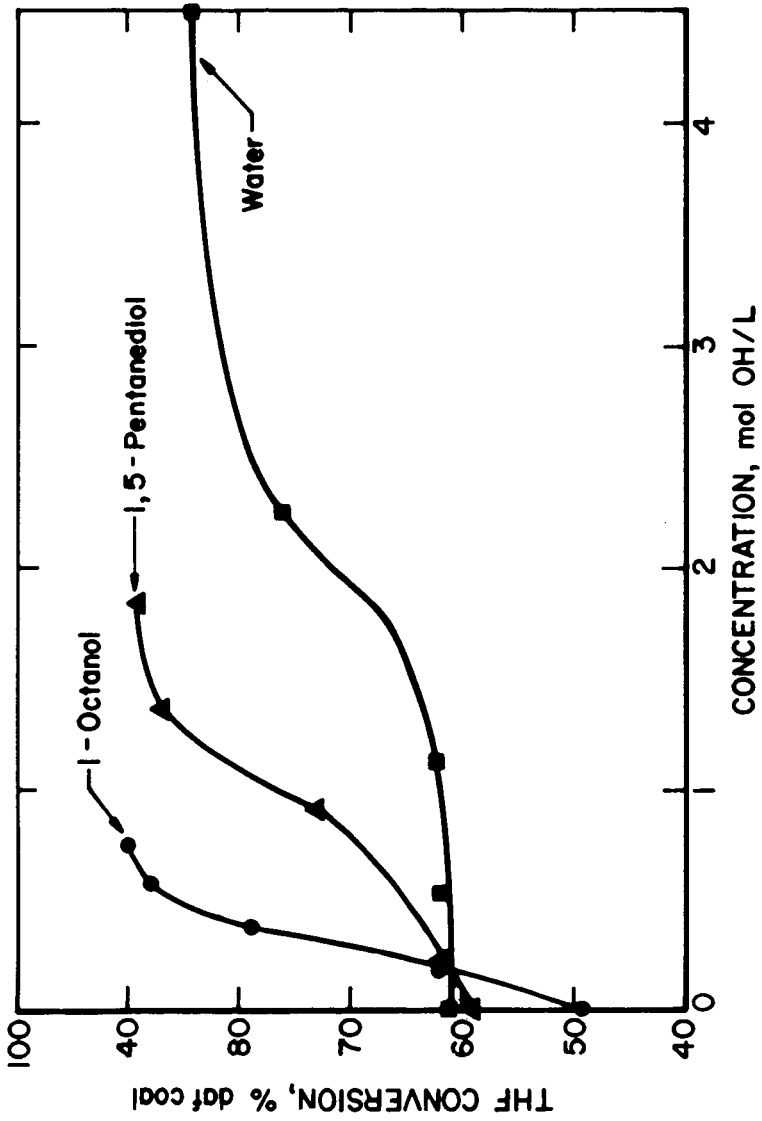


Fig. 5. Conversion in 1,2,4-Trimethylbenzene

INTRINSIC VISCOSITY OF LIGNITE-DERIVED PREASPHALTENES AND MODEL COMPOUNDS

J. K. Argasinski and M.B. Jones

Department of Chemistry, University of North Dakota
Box 7185 University Station, Grand Forks, ND 58202

INTRODUCTION

Non-covalent intermolecular interactions of coal-derived liquids have been studied by several researchers, particularly with respect to their effect on physical properties such as solubility and viscosity (1). Hydrogen bonding has been implicated in a number of studies as the principal attractive force responsible for the relatively high viscosity of coal asphaltenes (A) and preasphaltenes (PA) at ambient temperatures (2-10). For example, Bockrath and coworkers have reported that the viscosity of asphaltene solutions is predominantly a function of the phenol content (representing hydrogen bonding) and secondarily a function of molecular weight (representing van der Waals interactions) (4). Likewise, Tewari, et al., from studies of coal liquids (5,6) and model compounds (6) have demonstrated the importance of hydrogen bonding, largely involving phenolic OH and nitrogen bases, to the viscosity of coal liquids. Additional evidence for the importance of hydrogen bonding has been provided by derivatization studies. Gould and coworkers reported four- to seven-fold decreases in the viscosity of silylated coal liquefaction bottoms relative to the non-derivatized bottoms (9). Patel, et al. found a substantial increase in the dissolvability of solvent-refined lignite in nonpolar solvents after silylation or acetylation (10). The results of both investigations were interpreted in terms of disruption of intermolecular hydrogen bonding. Preasphaltenes have a greater impact on viscosity than do asphaltenes (3,7,9), but whether this is attributable to the larger molecular weight of the former (7) or to differences in concentrations of phenolic functionalities is not clear.

In connection with studies of intermolecular attractive forces in coal-derived liquids (12,13), we have measured the intrinsic viscosities of more than 60 model compounds and 6 lignite-derived preasphaltenes in THF solution. The goal of this project was to use well defined model compounds to assess the importance of various structural features, including molecular weight, functionality, and degree of aromatic condensation, to the intrinsic viscosity of the preasphaltenes.

EXPERIMENTAL

Total liquefaction samples were obtained from the University of North Dakota Energy Research Center. Details regarding the liquefaction conditions and yields and characterization of the preasphaltenes are given in Table 1. A modified version of the solvent extraction procedure of Steffgen, et al. (14) was used to separate the preasphaltenes (THF soluble, toluene insoluble) from the total liquefaction samples. Room temperature acetylations of preasphaltenes from runs 80 and 99 were accomplished following the method of Baltisberger, et al. (15). Both native and acetylated preasphaltene samples were separated into narrow molecular size fractions by preparative gel permeation chromatography (GPC) on Biobeads S-X3 or S-X8. Model compounds employed were either commercially available or were prepared by standard literature methods.

Specific viscosities of the preasphaltene samples and model compounds were measured in THF solution at 20 °C in Canon-Fenske flow-type viscosimeters. Intrinsic viscosities were calculated by extrapolation of plots of specific viscosities/concentration vs. concentration to infinite dilution. Viscosity and molecular weight data for selected model compounds and separated preasphaltene samples are presented in Table 2.

RESULTS AND DISCUSSION

Intrinsic viscosities were determined for THF solutions of lignite-derived preasphaltene samples from six different liquefaction runs (Table 1). The values obtained are quite similar, despite differences in processing conditions. The two samples with the highest intrinsic viscosities were those with the lowest carbon content and the highest oxygen content. One may be tempted to interpret these results in terms of the influence of polar oxygen functionalities in the preasphaltenes. However, GPC analysis of the preasphaltene samples revealed that the highest average molecular weights were exhibited by those same two samples. Thus, one may also suggest that the slight differences observed in the measured intrinsic viscosities may be ascribed to differences in molecular weight, and hence, nonspecific interactions such as van der Waals forces. Recent work by White and Schmidt has revealed the existence of a linear relationship between the average molar polarizability of Wilsonville and H-Coal liquefaction product distillates (boiling points from 400-900°F) and the mid-boiling point of those same distillates (16). Since the mid-boiling point is representative of the total intermolecular forces and polarizability is directly related to van der Waals forces, the authors concluded that the dominant intermolecular force in these distillates was van der Waals forces.

Because of the complexity of the preasphaltene samples, model compounds were employed to address the question of the relative importance of specific interactions such as hydrogen bonding and charge-transfer versus nonspecific interactions such as van der Waals forces to the intrinsic viscosity of the samples. The model compounds were chosen to evaluate four principal structural features: degree of aromatic condensation (representative of charge-transfer), aromatic carbon content (charge-transfer), hydrogen bonding functionalities, and molecular weight (representing the nonspecific interactions). Table 2 contains the intrinsic viscosity data for approximately half of the model compounds used in the study. The influence of aromatic condensation can clearly be seen by comparison of naphthalene with tetralin or decalin, phenanthrene with bibenzyl and perylene with 1,1'-binaphthyl. For each pair, the molecular weights are comparable, yet the more highly condensed aromatic compound possesses a greater intrinsic viscosity. Likewise, the aromatic carbon content influences the intrinsic viscosity. Compare, for example, tetraethylpyrene with perylene. The former is 62 g/mole heavier than the latter, but has a smaller intrinsic viscosity. This is likely due to the ethyl groups of tetraethylpyrene sterically interfering with stacking interactions of the aromatic nuclei. Both the degree of condensation and the aromatic carbon content apparently contribute to the intrinsic viscosity via charge-transfer interactions of the aromatic rings. The importance of hydrogen bonding functionalities to intrinsic viscosity is more pronounced than either of the two previous structural features. As expected, NH species exhibit a decreased effect in comparison to OH species (cf. 1,2,3,4-tetrahydroquinoline vs. tetralin with 2-naphthol vs. naphthalene). An increase in the number of hydrogen bond donating groups leads to a concomitant increase in intrinsic viscosity that is much larger than could be expected on the basis of an increase in molecular weight alone (cf. 2,7-naphthalenediol with 2-naphthol). The influence of molecular weight is perhaps best noted by comparisons of polystyrene oligomers. These samples differ in molecular weight without differing in aromatic condensation or aromatic carbon content (weight percent). Thus the observed differences in intrinsic viscosity may be attributed solely to differences in molecular weight and hence, nonspecific forces.

Assessment of the relative importance of specific vs. nonspecific forces is difficult and clouded by the fact that in most cases, an increase in the degree of condensation, aromatic carbon content, or number of hydrogen bonding moieties is accompanied by an increase in molecular weight. A potential approach to this dilemma is to use the Mark-Houwink equation ($[\eta] = KM^a$), which polymer chemists employ to relate molecular weight to intrinsic viscosity. Plots of the logarithmic form of this equation for the model compounds are presented in Figure 1A. The slopes of the least-squares lines for each data set correspond to the value of a in the Mark-Houwink equation. Model compounds which differ primarily in molecular weight alone yield a significantly smaller a value than model compounds which differ in

molecular weight and possess the capability of some specific interaction, either hydrogen bonding or charge transfer. Thus, one would suggest that contributions arising from specific forces outweigh those from nonspecific forces.

An analogous argument may be applied to the preasphaltene samples. Separation of two total preasphaltene samples into narrow molecular weight fractions was accomplished by preparative GPC. A logarithmic Mark-Houwink plot of the preasphaltene data is given in Figure 1B. For both the native and acetylated samples of PA-80, the value of a is closer to that obtained from the model compounds which exhibit specific interactions. On the other hand, the a -values for the samples of PA-99 are similar to that of the nonspecific interaction model compounds. Therefore, the individual preasphaltene samples do not appear to be uniform in the structural features which play a crucial role in determining intrinsic viscosity. As in many cases involving coal liquids, generalization regarding intrinsic viscosity may not be appropriate.

Comparison of molar volumes of the model compounds and separated preasphaltenes calculated from intrinsic viscosity with molar volumes calculated from density affords a semi-quantitative measure of the interaction of the solute with the solvent (THF). These data are reported in Table 2 as n_{THF} . Hydrogen bonding with the solvent is clearly identifiable for low molecular weight model compounds with phenolic functionalities (cf. naphthalene, 2-naphthol, 2,7-dihydroxynaphthalene). Other functional groups (OR, NH) also cause association beyond that expected on the basis of size alone. Functional group contributions to THF association may be determined from these data to be 1.0 THF molecule per OH, 0.4 THF/OR and 0.2 THF/NH. Without question, however, as the molecular weight increases, the dominant contributing factor to THF association is molecular size. This can readily be seen for both the model compounds and the preasphaltene samples in Figure 2.

Acknowledgements

The authors gratefully acknowledge the financial support of the U.S. Department of Energy (Grant No. DE-FG-22-83PC60808) and the University of North Dakota Energy Research Center for providing total liquefaction samples and analytical data. Discussions with Professors R.J. Baltisberger, N.F. Woolsey and V.I. Stenberg and Dr. Curt White were very useful. We thank Professor Woolsey for the sample of tetraethylpyrene.

REFERENCES

1. See, for example, Stenberg, V.I., Baltisberger, R.J., Patel, K.M., Raman, K. and Woolsey, N.F. in "Coal Science"; Gorbaty, M.L., Larsen, J.W. and Wender, I., Eds.; Academic Press: New York, 1983; Vol. 2, Chapter 3.
2. Stenberg, H.W., Raymond, R. and Schweighardt, F.K. *Science* 1975, **188**, 49.
3. Bockrath, B.C., LaCount, R.B. and Noceti, R.P. *Fuel Process. Technol.* 1977/1978, **1**, 217.
4. Bockrath, B.C., LaCount, R.B. and Noceti, R.P. *Fuel* 1980, **59**, 621.
5. Tewari, K.C., Hara, T. Young, L-J.S. and Li, N.C. *Fuel Process. Technol.* 1979, **2**, 303.
6. Tewari, K.C., Kan, N-S., Susco, D.M. and Li, N.C. *Anal. Chem.* 1979, **51**, 182.
7. Young, L-J.S., Hara, T. and Li, N.C. *Fuel* 1984, **63**, 593.
8. Young, L-J.S. Yaggi, N.F. and Li, N.C. *Fuel* 1984, **63**, 816.
9. Thomas, M.G. and Granoff, B. *Fuel* 1978, **57**, 122.
10. Gould, K.A., Gorbaty, M.L. and Miller, J.D. *Fuel* 1978, **57**, 510.
11. Patel, K.M., Stenberg, V.I., Baltisberger, R.J., Woolsey, N.F. and Klabunde, K.J. *Fuel* 1980, **59**, 449.
12. Jones, M.B. and Argasinski, J.K. *Fuel* 1985, **64**, 1547.
13. Jones, M.B. and Argasinski, J.K. *Am. Chem. Soc., Div. Fuel Chem., Prepr.* 1985, **30(4)**, 250.
14. Steffgen, F.W., Schroeder, K.T. and Bockrath, B.C. *Anal. Chem.* 1979, **51**, 1164.
15. Baltisberger, R.J., Patel, K.M., Woolsey, N.F. and Stenberg, V.I. *Fuel* 1982, **62**, 848.
16. White, C.M. and Schmidt, C.E. submitted to *Energy and Fuels*.

TABLE 1. Coal liquefaction conditions and preasphaltene (PA) characterization.^a

Run no.	Temp. (°C)	Press. (MPa)	Additive	Yield PA ^b	Analysis ^c					Intrinsic viscosity
					C	H	N	S	O ^d	
80	456	22	H ₂ S	10.7	77.8	6.1	2.1	0.7	13.3	3.90
89	436	19	H ₂ S	9.0	81.6	5.6	2.6	0.6	9.6	3.78
90	436	15	-	11.2	83.8	5.4	2.3	0.3	8.2	3.63
93	440	15	S	8.6	81.9	5.5	2.5	0.6	9.5	3.57
98	440	14	H ₂ S + pyrite	6.2	81.2	5.7	2.6	0.6	9.9	3.52
99	400	16	-	19.6	80.1	5.7	2.1	0.4	11.7	3.99

^aAll runs were carried out with Big Brown Texas lignite under bottoms recycle operation with H₂-CO as the reducing gases

^bYields are based on starting weight of total coal liquefaction product

^cWeight percent

^dBy difference

Table 2. Intrinsic viscosities and THF association of selected model compounds and separated preasphaltene samples.

Compound	MW	$[\eta]^a$	n_{THF}^b
Benzene	78	0.24	0.1
Naphthalene	128	1.43	1.0
Biphenyl	154	1.54	1.3
Phenanthrene	178	1.94	1.9
Chrysene	228	2.34	2.9
1,1'-Binaphthyl	254	2.30	3.2
Perylene	252	2.64	3.7
Diphenylmethane	168	1.40	1.3
Fluorene	166	1.64	1.5
Bibenzyl	182	1.58	1.6
1-Methylnaphthalene	142	1.22	1.0
2,6-Dimethylnaphthalene	156	1.30	1.1
Tetralin	132	1.15	0.9
Decalin	138	1.02	0.8
1,3,6,8-Tetraethylpyrene	314	1.93	3.5
1-(2-Naphthalenylmethyl)pyrene)	342	2.91	5.4
Carbazole	167	2.13	2.0
Quinoline	129	1.51	1.1
5,6,7,8-Tetrahydroquinoline	133	1.20	0.9
1,2,3,4-Tetrahydroquinoline	133	1.81	1.3
2-Naphthol	144	2.58	2.0
2,7-Naphthalenediol	160	4.11	3.6
2-Methoxynaphthalene	158	1.60	1.4
2-Naphthol acetate	186	1.61	1.7
2,7-Naphthalenediol diacetate	244	2.11	2.8
4,4'-Biphenol	186	4.22	4.3
4,4'-Biphenol diacetate	270	2.35	3.4
1-Pyrenol	218	2.88	3.5
Pentaphenyl ether	446	2.77	6.8
Polystyrene	615	2.68	9.3
Polystyrene	1140	3.45	22.4
Polystyrene	2500	4.90	69.0
Poly(2-vinylnaphthalene)	570	3.24	9.8
Poly(2-vinylnaphthalene)	1150	3.96	25.1
PA-80-1N	1202	7.53	50.0
PA-80-2N	470	2.90	8.0
PA-80-3N	375	1.85	4.7
PA-80-4N	272	1.88	3.1
PA-80-1A	1077	5.31	32.4
PA-80-2A	605	2.58	9.3
PA-80-3A	520	2.38	7.7
PA-80-4A	313	1.55	3.2
PA-99-1N	1382	5.32	40.0
PA-99-2N	584	4.13	13.1
PA-99-3N	443	3.77	9.3
PA-99-4N	337	3.58	6.8
PA-99-1A	1080	4.35	28.2
PA-99-2A	614	3.46	11.8
PA-99-3A	478	2.93	7.7
PA-99-4A	370	2.82	5.6

^aIntrinsic viscosity

^bNumber of THF molecules associated with one molecule of compound

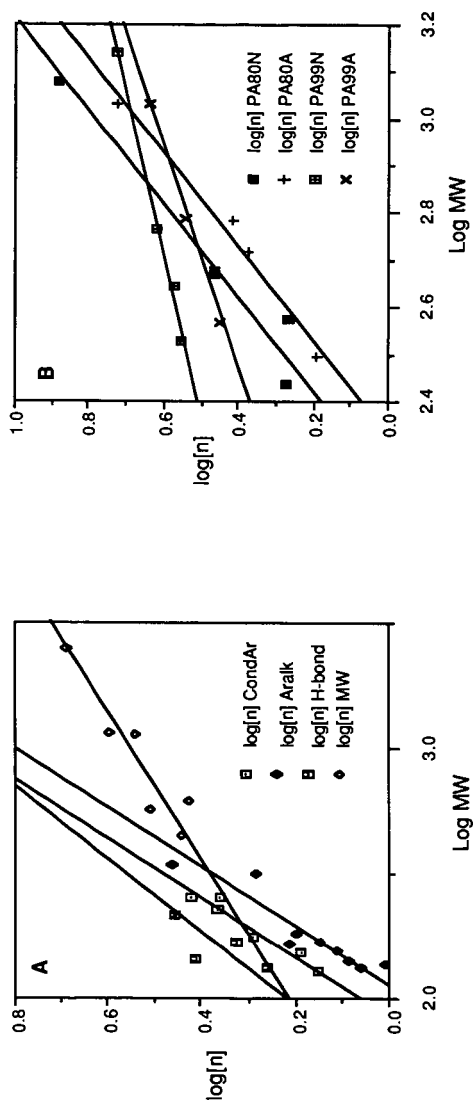


Figure 1. Plots of log intrinsic viscosity ($[\eta]$) vs. log molecular weight for selected model compounds and separated preasphaltenes. (A) CondAr = condensed aromatic models, Aralk = alkyl- and hydroaromatic models, H-bond = model compounds with one functional group capable of hydrogen bonding with THF, MW = polystyrene and poly(2-vinylnaphthalene models. (B) N = native (nondenaturated), A = acetylated.

"NEW FUELS" VIA DIRECT COAL LIQUEFACTION

ENE0 C. MORONI

U.S. Department of Energy, FE-34 GTN, Washington, D.C. 20545

INTRODUCTION

This paper is part of a series of papers (1-4) directed to inform the research community of the major achievements obtained during the development of the Integrated Two-Stage Liquefaction (ITSL) process and recent results from a few research laboratories which are closely related to the ITSL approach. The conclusion derived from these achievements is that the low-severity approach, exemplified by the ITSL process, has shaped a new direction in direct coal liquefaction development which needs further complementary support work of manifestly fundamental nature.

This paper intends to demonstrate that low-severity coal liquefaction operations are instrumental in producing some uniquely structured hydrocarbon distillate products. While the structure of these hydrocarbons can be traced to the unique condensed cyclic hydrocarbon structure present in coals, the low-severity operations, practiced in staged coal liquefaction processes, are the main contributors to the maintenance of the cyclic structure throughout and up to the final distillate products.

LOW-SEVERITY OPERATIONS

The ITSL and Chevron Two-Stage Coal Liquefaction processes have been described previously in detail (5-7) and they are representative of the novel low-severity staged operation approach which have shown to yield mostly reactive low-molecular-weight fragments (8). Other low-severity staged processes have been reported in the literature but bench-scale efforts were never conducted to a steady-state or a fully integrated operations, from which the required material and energy balances can be secured.

The staged process approach is based on the fact that there are two distinct paths - thermal and catalytic - to efficient coal liquefaction for obtaining "meaningful" fuel products and that the two must be separated because they have quite different, almost opposite, optimum operating conditions.

In the first stage coal and hydrogen donor solvent are reacted under hydrogen gas overpressure to form an "adduct" between coal and solvent. If the quality of the hydrogen donor solvent is excellent, as measured by proton NMR (9), practically no gaseous hydrogen is consumed and the resultant adduct contains exactly the arithmetic average of hydrogen available in the two components, i.e., solvent and coal mixed in a S/C ratio of 1.8 and containing 8.0-8.5 and 4.5-5.0 weight percent hydrogen, respectively, form an adduct with 6.5-7.2 weight percent hydrogen.

Since the best hydrogen donor solvent seems to be produced by "catalytic" hydrogenation at about 400°C in the ITSL second stage, the donor solvent is efficiently dehydrogenated in the "thermal" first stage at temperatures well above 400°C. No hydrogen loss from the donor solvent to gas phase is observed because of the hydrogen gas overpressure in the reactor.

The high temperature required in the thermal first stage serves also to convert efficiently coal preasphaltenes and asphaltenes to oils. It is fortunate that these conversions are very fast and the short reaction time provides the low-severity operations required to avoid retrogressive reactions. The optimum short contact time is of the order of 2-3 minutes, measured from the reactor inlet temperature of 320°C to the outlet at 440-450°C.

The coal extract produced in the first stage has been shown (6) to be more suitable than SRC I extract for the depolymerization occurring in the catalytic second stage. The low-severity operation in the second stage is maintained by limiting the reaction temperature at 400°C or below.

There are several reactions occurring in the catalytic second stage. The three most important are: 1. the hydrogenation of the solvent; 2. the removal of the heteroatoms, and 3. the depolymerization of the condensed aromatic compounds.

The requirements of this operation are to maximize the hydrogen donor quality of the recycle solvent and the removal of heteroatoms, while limiting the depolymerization to "controlled" ring opening without destroying the cyclic nature of the distillate ultimately produced. All these reactions have to be carried out with the minimum consumption of hydrogen and with a catalytic-bed reactors adsorbing about one million BTU per ton of coal processed owing to the highly exothermic hydrogenation reaction. Moreover, the required overall material balance involving hydrogen, recycle solvent and distillate product balances must be reached and maintained for a successful integrated continuous operation, even though there is a continuous declining catalyst activity.

Asking for all these required tasks to be accomplished in a single catalytic reactor seems to be asking the impossible. And yet by using an expanded catalytic bed reactor, similar to the commercial H-Oil reactor used in petroleum refineries, most of the task requirements are met.

On the other hand, there are many reactions occurring in the second stage which could be partially, if not totally, accomplished in the first stage, taking the workload away from the second stage. In the latter, more emphasis could be focused to produce better donor solvent and distillate product qualities. Of the total distillate coming out of the catalytic second stage the -343°C (-650°F) fraction, corresponding to the overhead fraction of the atmospheric flash distillation, was selected as the optimal product for being environmentally acceptable and already in the gasoline, diesel and jet fuel boiling range, as shown in Figure 1, and be upgraded to specification transportation fuels using modern commercial petroleum-processing technology.

Figure 1 shows typical distillation curves of several coal-derived oils compared to that of an Arabian-light petroleum crude. One notices significant differences between the ITSL distillate and the petroleum crude as well as the other coal liquids. In particular, the ITSL distillate contains a much larger middle distillate fraction (76 volume percent boils between 200° and 350°C), and less naphtha than coal-derived oils produced at higher-severity process conditions.

It is thought that this unique characteristic of the ITSL distillate supports the claim of being able to produce coal derived "New Fuels" that are significantly different from distillate derived from petroleum crudes.

The ITSL distillate has been refined successfully in a prototype refinery (10) using modern refining technology to produce specification transportation fuels with distinctive advantageous features, as will be described later.

NEW FUELS

Owing to the condensed cyclic structure of coal, the majority of the distillate products obviously will contain mostly condensed cyclic compounds, no matter what liquefaction approach is used. However, coal liquefaction at high-severity operations yield large quantities of light naphtha which, in most instances, contain above 45 volume percent of paraffins (11). Needless to say, converting condensed and non-condensed aromatics to paraffins requires the unnecessary consumption of hydrogen and is an indication of operations that are not optimally controlled.

On the other hand, low-severity liquefaction processes are able to depolymerize coals to low-molecular weight distillates that consist almost exclusively of cyclic compounds. To underline the importance of this extra-ordinary selectivity the enclosed table shows the product yield structure of the nominal boiling point to -350°C distillates produced by the ITSL process in which only mono- to condensed tri-cyclic compounds are present, no matter which type of coal is used, bituminous Illinois No. 6, Burning Star Mine or subbituminous Wyodak, South Pit Mine. Furthermore, one can observe that there are no condensed tetracyclics and, for the bituminous coal, no paraffins. It seems likely that the paraffins found in the distillate fraction of the subbituminous coal, probably were derived from the original structure of the coal, rather than being formed at low-severity operations. This assumption needs to be confirmed by a more precise characterization of the paraffinic species in the original coal and by monitoring their possible conversion to lower-molecular weight paraffins, either in the thermal or the catalytic stage of processing.

Figure 2 shows the comparative true boiling point curves of the ITSL atmospheric flash distillates from Wyodak and Illinois No. 6 coals, which reveals higher boiling compounds in the middle-distillate range for the Wyodak coal. The results were unexpected since subbituminous coal contains, on the average, lower molecular-weight condensed aromatic clusters and data from the H-Coal distillates from the same two coals have shown much lower boiling curves for Wyodak than for Illinois No. 6 coal (11). It should be noted that the H-Coal process operated at the same conditions for the two coals, whereas in the ITSL's catalytic second stage operations for Illinois No. 6 were conducted at 400°C and for the Wyodak coal at 370°C. From these results one might conclude that the distillate product yield distribution, in this case the condensed tri-bi and monocyclic ratios, can be

modified by changing processing conditions - a very desirable feature of controlled processing flexibility.

The fact that we can produce distillates from coal containing almost exclusively selected cyclic hydrocarbons, and can modify, under controlled conditions, their ratios within a selected boiling range is indeed one of the most important achievements in direct coal liquefaction R&D.

Another very important point is that these uniquely structured distillates have been characterized as "High Density Fuels," meaning that they provide greater energy per unit volume than do the more conventional fuels.

Figure 3 illustrates the selective conversion of coal to mostly bicyclic compounds such as naphthalenes, tetralins and decalins, representing about 50 percent of the total aromatics, hydroaromatics and naphthenes produced at low-severity operations, respectively. These "High Density Fuels" have different properties than petroleum-derived transportation fuels and can be considered as "New Fuels" with potential new applications. In addition, to provide desirable "more mileage per gallon fuels" and "lower freezing point" for jet fuels, these unique fuels can be produced at several levels of hydrogen to suit specific new engine requirements, and, possibly improve their performance.

Catalytic "hydrogenation" and "dehydrogenation" of these distillates require low activation energy of about 15 kcal/mole to produce, as desired, either naphthenes, or hydro-aromatics, or only aromatics, without breaking the original ring structure.

The versatility of the products as fuels can be appreciated if one notes the intrinsic properties of each of these products, whether they are condensed or non-condensed.

Naphthenes, upon heating prior to combustion, dehydrogenate to produce aromatics and large quantities of hydrogen providing a desirable strong "cooling" (endothermic) action in the precombustion zone. The mixture of hydrogen and aromatics is a highly desired fuel for recently developed high performance engines.

Hydroaromatics, alone, have never been tested as fuel. On the basis of their behaviour as "rapid hydrogen donors" in coal liquefaction they could provide hydrogen plus aromatics at a faster rate than naphthenes, if this would be a desirable feature.

Aromatics would provide higher combustion temperatures than naphthenes and hydroaromatics and could be suitable for newly introduced engines, i.e., ceramic engines, although soot formation problems need to be solved for this type of fuel. An all-aromatics fuel would be the least expensive to produce since it would require the least hydrogen addition in coal processing and refining steps.

CONCLUDING REMARKS

It is imperative to promote the development of these new fuels and eventually other forms of fuels from coal, presently in the exploratory research stage, by exploiting their unique properties.

They have the potential to create their own special fuel market aside from-- as well as in combination with--petroleum fuels.

Consequently, supportive funding for the development of new fuels from coal should not be negatively affected by the current low cost of petroleum.

REFERENCES

1. E. C. Moroni, "Direct Coal Liquefaction: New R&D Direction" Proceedings 1985 International Conference on Coal Science, Sydney, Australia, October 28-30, 1985, p. 47
2. E. C. Moroni, "Bridging the Gap Between R&D and Commercial Feasibility" Preprints ACS, New York, New York, April 13-18, 1986, Division of Fuel Chemistry, Vol. 31, No. 2, p. 340
3. E. C. Moroni, "Integrated Two-Stage Liquefaction: The Legacy and Unfinished Work." ACS National Meeting, Anaheim, California
4. E. C. Moroni, "Low-Severity Coal Liquefaction: A Challenge to Coal Structure Dependency." ACS National Meeting, Anaheim, California, September 7-12, 1986
5. H. D. Schindler, J. Chen and J. Potts, "Integrated Two-Stage Liquefaction" Final Technical Report - Volume I, July 1985, Lummus-Crest, Inc./DOE Contract PC 50021, Q 11
6. M. B. Neuworth and E. C. Moroni, "Development of an Integrated Two-Stage Coal Liquefaction Process" Fuel Processing Technology, 8(1984) 231-239, Elsevier Science Publishers
7. J. W. Rosenthal, A. J. Dahlberg, C. W. Kuehler, D. R. Cash and W. Freedman, "The Chevron Coal Liquefaction Process" - 47th API Midyear Refining Meeting - Synfuel Processes, New York, New York, May 12, 1982
8. J. H. Shinn, "From Coal Single-Stage and Two-Stage Products: A Reactive Model Coal Structure." Fuel, Vol. 63, 1187, 1984
9. R. A. Winschel and F. P. Burke, "Recycle Slurry Oil Characterization" First Annual Report - October 1, 1980 through September 30, 1981. DOE Contract No. PC 30027-24, July 1982
10. R. F. Sullivan and H. A. Frumkin, "Refining Coal Liquids: Where We Stand." Preprints ACS National Meeting, New York, New York, April 13-18, 1986. Division of Fuel Chemistry, Vol. 31, No. 2, p. 325
11. R. F. Sullivan, "Refining and Upgrading of Synfuels from Coal and Oil Shales by Advanced Catalytic Process" Fifth Interim Report - H-Coal - September 1981 DOE/ET 10532-T3 and Fifth (Addendum) Interim Report - H-Coal, May 1982, FE-2315-77

TRUE BOILING POINT DISTILLATIONS FOR ARABIAN LIGHT CRUDE, SHALE OIL AND COAL-DERIVED SYNCRUDES

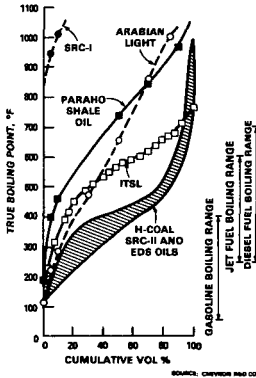


FIGURE 1

**ITSL DISTILLATE PRODUCTS
NOMINAL — 650°F**

	ILLINOIS NO 6 WOW 4998	WYODAK SGQ 9774
PARAFFINS	0.0	3.7
MONOCYCLICS	26.3	16.4
BICYCLICS	50.5	48.3
TRICYCLICS	21.6	29.5
TETRACYCLICS	0.0	0.0
TOTAL HYDROCARBONS	98.4	97.9

SOURCE: CHEVRON R&D CO.

**COMPARISON OF 725--750°F END POINT
WYODAK AND ILLINOIS ITSL OIL PILOT PLANT FEEDS
(ASTM D 2887 DISTILLATIONS)**

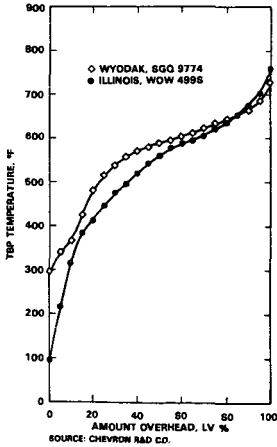


FIGURE 2

VERSATILE "NEW FUELS" FROM COAL

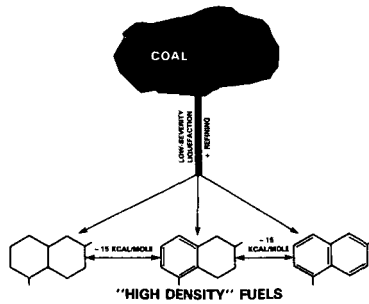


FIGURE 3

CATALYTIC HYDROCRACKING OF TAR VAPOURS IN HYDROPYROLYSIS

C. Bolton and C.E. Snape

British Coal, Coal Research Establishment,
Stoke Orchard, Cheltenham, Glos., GL52 4RZ, UK.

H.P. Stephens

Sandia National Laboratories, Albuquerque, New Mexico, 87185

ABSTRACT

Tar vapours have been hydrotreated in the second stage of a fixed-bed two-stage hydropyrolysis reactor using hydrous titanium oxide catalysts exchanged with Ni, Co, Mo and Pd and a commercially available Ni/Mo on alumina catalyst. The primary tar, which accounted for 25-30% daf coal (UK bituminous, 82% dmmf C) was converted at 400°C and 150 bar to a colourless liquid low in heteroatoms of which up to 40% boiled below 150°C. The gas yield was only slightly higher than that obtained in corresponding single-stage tests. A lower boiling product was obtained with Ni/Co/Mo hydrous titanium oxide than with the commercial Ni/Mo catalyst. The most extensively hydrogenated product was obtained with Pd which was still effective at 300°C and 50 bar. The initial effects of carbon build-up on product composition are similar for the alumina- and hydrous titanium oxide-Ni/Mo catalysts tested.

INTRODUCTION

Thermal decomposition of coal under hydrogen pressure (hydropyrolysis) (1-3) is a possible route to chemical feedstocks and synthetic fuels. Tar yields are significantly higher than those obtained by conventional carbonisation. Above about 750°C, primary tars hydrocrack to give appreciable yields of benzene and ethane (3,4). Unfortunately, methane yields and, consequently, hydrogen consumptions are also high. However, tar vapours can be catalytically hydrotreated at about 400°C to give distillable liquids although, in early studies (5-7), the yields were low (<10% daf coal) principally because the reactors were operated at relatively low pressure (<50 bar). Recently, much higher yields of low boiling products (20-25% daf coal) with little methane have been obtained in a two-stage fixed-bed reactor operated at 150 bar (8) and using a commercial Ni/Mo catalyst.

Previous work by one of the authors has demonstrated that hydrous titanium oxide (HTO) exchanged with Pd can hydrogenate polynuclear aromatic compounds at much lower temperatures and pressures than conventional Ni/Mo and Co/Mo on alumina catalysts (9,10). In the present study, HTO formulations containing Ni, Co, Mo and Pd have been used to hydrotreat tar vapours in two-stage hydropyrolysis. The results are compared with those obtained previously using a commercial Ni/Mo catalyst (8).

EXPERIMENTAL

Coal

The proximate and ultimate analyses of the high volatile UK bituminous coal used are listed in Table 1.

Catalysts

The HTO catalysts belong to a group of alkoxide-derived amorphous ion-exchange compounds represented by the empirical formula $(C^X M^Y O^Z H)$, where C is an exchangeable cation and M is either Ti, Zr, Nb or Ta. Six catalysts containing Ni, Co, Mo and Pd and combinations of these were prepared by the method

described previously (11,12) The compositions and some properties of these formulations, together with those of the commercial Ni/Mo catalyst used for comparison, are given in Table 2.

Powdered catalyst was made into discs (35 mm dia. by 3 mm thick) in a press operated at 690 bar. The discs were crushed and sieved to obtain the 0.5-1.7 mm fraction. All but the Pd catalyst were pre-sulphided with 10% H₂S in hydrogen at 400°C and atmospheric pressure. Most of the tests were performed with catalyst pre-sulphided prior to loading into the reactor. However, the Ni/Co/Mo HTO and the commercial Ni/Mo catalysts were also pre-sulphided in-situ.

Apparatus and procedure

The apparatus shown schematically in Figure 1 is similar to that described previously (8). Hydrogen under pressure flows downwards through the reactor tube. Coal in the upper section is heated resistively, the temperature of the hydrolysis zone being monitored by a thermocouple in the coal bed. The lower section heated by a muffle furnace is used for hydrotreating of tar vapours. Liquid products, including water, condense in the dry ice trap. Two-stage hydrolysis was normally carried out at 150 bar pressure with pyrolysis and hydrotreating temperatures of 500° and 400°C respectively. However, the more promising catalyst formulations were also tested under less severe conditions, namely at 300°C and 50 bar, the hydrolysis temperature being raised to 575°C to maintain the same tar yield. 10 g of vacuum dried coal (250-500 μm) mixed with 20 g of sand and 8 g of catalyst were placed in their respective zones in the reactor. The hydrolysis zone was heated at a rate of 5°C/s from ambient and held at the desired temperature for 10 minutes. A hydrogen flow equivalent to 5°C/min. at normal temperature and pressure was used giving an estimated residence time of 10 s for tar vapours in the catalyst bed. Deactivation experiments were carried out by using the Ni/Mo HTO and alumina catalysts in six consecutive passes. To accelerate carbon build up, the ratio of coal to catalyst was increased to 3:1 (15 g of coal).

Product recovery and analysis

Gas, liquid and char, as well as the catalyst, were recovered for analysis. Much of the liquid product that collected in the cold trap could be drained out, the remainder being recovered with ether. Water was removed from the liquid products using phase separating paper. Some of the used catalysts were Soxhlet extracted with dichloromethane (DCM) to remove any trapped product.

¹H NMR and elemental analyses and enthalpimetric titrations (13) to determine acidic OH concentrations were carried out on the liquid products. Concentrations of low boiling constituents were determined by GC using a squalane capillary column and iso-butylbenzene as internal standard. Carbon and, in some cases, sulphur contents of the recovered and DCM-extracted catalysts were determined. Concentrations of trapped product in the used catalysts from the deactivation experiments were estimated from the weight loss up to 500°C.

RESULTS AND DISCUSSION

Previous work (8) using a single-stage reactor at 500°C and 150 bar, showed that between 25 and 30% tar was obtained from Linby coal while the hydrocarbon gas yield was only 5%. This work also showed that, although the tar yield increased with temperature up to about 650°C, the gas yield increased much faster e.g. at 600°C, the tar yield had reached 35% but the hydrocarbon gas yield had risen to 18%, including 10% methane.

In the present work the fresh catalysts tested at 400°C and 150 bar yielded 20±3% colourless liquid product (Table 3), while gas yields were only slightly higher than those obtained in the equivalent single-stage hydrolysis tests (8). The liquids contain up to 40% boiling lower than about 150°C, the major

constituents being alkylcyclohexanes, alkylbenzenes and alkanes (Figure 2 and Table 4). ¹H NMR indicates that the concentrations of naphthalenes and other di-aromatic species are low (Figure 3 and Table 5). Nitrogen-containing compounds and phenols are only minor constituents (Table 5). (Reliable sulphur values could not be determined possibly due to the presence of elemental sulphur released from the fresh catalysts.)

The Pd HTO catalyst gave the most hydrogenated liquid product, the aromatic hydrogen content (Table 5) and ratios of benzene to cyclohexane and toluene to methylcyclohexane (Table 4) being the lowest achieved. The extent of hydrogenation was greater for the pre-sulphided Ni/Mo on alumina catalyst than for the other HTO catalysts tested. The Ni/Co/Mo formulation pre-sulphided in-situ gave the most aliphatic product.

The light naphtha yields given in Table 4 provide a convenient comparison of catalyst hydrocracking ability, the highest yield being obtained with the Ni/Co/Mo HTO catalyst pre-sulphided in-situ; it is uncertain why the method used to pre-sulphide this catalyst affects both the extent of hydrogenation and hydrocracking. Light naphtha yields for the Ni/Mo and Co/Mo HTO and Ni/Mo on alumina catalysts were similar. Interestingly, the Pd HTO catalyst gave a lower yield indicating that hydrocracking and hydrogenation abilities are not related.

The yields of liquid products obtained at 300°C and 50 bar pressure were lower (about 15%) than at 400°C (Table 3) because more tar remained on the catalysts (Table 6). The Ni/Co/Mo HTO catalyst was much less effective under the milder conditions giving a more aromatic and phenolic product (see Tables 4 and 5). In contrast, the product obtained with the Pd catalyst was similar to that obtained at 400°C, BTX concentrations being extremely low. The 300°C product contained more light naphtha probably because a greater proportion of the high MW constituents in the tar condensed on the catalyst bed. However, the initial build-up of carbon does not seem to impair the low temperature hydrogenating ability of the Pd catalyst (9,10).

All the catalysts gained carbon but the pre-sulphided catalysts also lost sulphur (Table 6). However, the recovered HTO catalysts contained less carbon than the corresponding commercial Ni/Mo catalyst. Soxhlet extraction with DCM removed between 2 and 3% material leaving as little as 1% carbon (equivalent to about 3% of the primary tar). Although the extracts were dark in colour, their acidic OH contents (1-2%) were significantly lower than that of the primary tar (about 5%, ref.8).

After a sharp initial rise during the first pass, there was a steady build-up of carbon on both the HTO and alumina Ni/Mo catalysts in the deactivation experiments (Table 6). However, the carbon content of the HTO catalyst was always lower. The amount of extractable material on the catalysts remained fairly constant after the first pass, about 3% DCM soluble material being recovered from both catalysts after the sixth and final pass.

Figure 4 summarises the changes in the composition of the liquid products as deactivation progressed. The products after the first pass had little colour but were more aromatic and contained less light naphtha than the corresponding products from the catalyst screening tests (Tables 4 and 5) because less catalyst and more coal was used. The products from the remaining passes were all dark in appearance and contained more nitrogen, acidic OH and aromatic hydrogen (Figure 4). The extent of hydrogenation remained fairly constant after the first pass (see aromatic hydrogen contents, Figure 4) but the heteroatom content continued to increase while the light naphtha yield decreased.

These results suggest that tar trapped on the catalysts is largely responsible for the initial deactivation but the slower build up of coke (non-extractable material) continues to reduce the extents of heteroatom removal and of hydrocracking. The level of deactivation appears to be fairly similar for the HTO and alumina catalysts tested (Figure 4) taking into account that the alumina catalyst initially gave the more hydrogenated product.

CONCLUSIONS

1. Hydrous titanium oxide catalysts are capable of upgrading tar vapours to give low boiling products.
2. Pd and Ni/Co/Mo hydrous titanium oxide catalysts are particularly promising. Pd gave a more extensively hydrogenated product and Ni, Co, Mo, a lower boiling product than the commercial Ni/Mo catalyst. The Pd catalyst was still effective at 300°C.
3. The effect of deactivation on product composition was similar for Ni/Mo hydrous titanium oxide and alumina catalysts.

ACKNOWLEDGEMENT

The authors thank British Coal for permission to publish this paper. The views expressed are those of the authors and not necessarily those of British Coal.

REFERENCES

1. Gavalas, G.R., 'Coal Pyrolysis', Elsevier (1982).
2. Fynes, G., Ladner, W.R. and Newman, J.O.H., Prog. Energy Combust. Sci., 6, 223 (1980).
3. Furfari, S., IEA Report No. ICTIS/TR20 (1982).
4. Finn, M.J., Fynes, G., Ladner, W.R. and Newman, J.O.H., Fuel, 59, 397 (1980).
5. Perry, R.C. and Albright, C.W., US Patent No.3,231,486 (1966).
6. Flinn, J.F. and Sachsel, G.F., I and E.C. Proc. Des. and Dev., 7(1), 143, (1968).
7. Karr, C.Jr., Mapstone J.O. Jr., Little L.R. Jr., Lynch, R.E. and Comberlati, J.R., I. and E.C. Prod. Res. and Dev., 10(2), 204, (1971).
8. Snape, C.E. and Martin, T.G., Proc. of Round Table Meeting, Commission of the European Communities, Burssels, 12th December 1985, EUR 10588, p167.
9. Stephens, H.P. and Kottenstette, R.J., Prepr. Am. Chem. Soc. Div. of Fuel Chem., 30(2), 345 (1985).
10. Stephens, H.P. and Dosch, R.G., Proc. of 4th Int. Symp. on the Scientific Bases for the Preparation of Catalysts, Louvain-La-Neuve, Belgium, 1st Sept. 1986, in press.
11. Stephens, H.P., Dosch, R.G. and Stohl, F.V., I. and E.C. Prod. Res. and Dev., 24, 15 (1985).
12. Dosch, R.G., Stephens, H.P. and Stohl, F.V., U.S. Patent No.4, 511, 455 (1985).
13. Vaughan, G.A. and Swithenbank, J.J., Analyst, 90, 594 (1965).

TABLE 1 - Analyses of Linby Coal

NCB CRC	ISO Class	Proximate analysis			Ultimate analysis					
		% ar H ₂ O	% db Ash	% daf V.M.	C	H	O	N	S	Cl
802	811	9.8	6.9	37.9	83.0	5.5	8.7	1.9	1.5	0.45

TABLE 2 - Catalyst formulations and properties

Type	Active Metal Content (wt %) ^a	BET Surface Area (m ² /g)	Sulphur Content (wt %) ^{a,b}
HTO] 10.1 % Mo	84	3.8
] 10.0 % Ni	148	3.9
] 2.0 % Ni	174	5.4
] 12.2 % Mo		
] 1.7 % Co	135	6.1
] 12.8 % Mo		
] 1.2 % Co	148	6.2
] 1.0 % Ni		
] 12.3 % Mo		
] 15.7 % Pd	189	--
Alumina ^c	3.0 % Ni 15.0 % Mo	180	5.9

KEY
^a = Volatile-free basis
^b = Freshly presulphided catalyst
^c = Akzo 153

TABLE 3 Product yields from two-stage catalytic hydrolysis tests

Hydrotreating T°C	400				300			
	Ni	Mo	Ni/Mo	HTO	Alumina	Ni/Co/Mo	Ni/Co/Mo	HTO
Catalyst type	S	S	S	S	O	P	P	O
Active Metals								
Pre-sulphiding								
Char	63	63	62	63	63	64	63	61
Liquid Product	21	23	21	23	19	20	22	15
Total gas ^a	7	7	8	7	8	7	7	11
Methane	3.0	3.0	3.6	2.7	4.3	3.4	3.7	6.1
								7.0

KEY ^a = C₁-C₄ hydrocarbons, CO₂ and CO

S = beforehand

P = in-situ

O = not pre-sulphided

TABLE 4 GC analysis of light naphtha fractions

Hydrotreating T°C	400			300							
	HTO	Co/Mo	Alumina	HTO	Co/Mo	HTO					
Catalyst type	NI	Mo	NI/Mo	Co/Mo	NI/Co/Mo	NI/Co/Mo					
Active metals	S	S	S	S	S	P					
Pre-sulphiding											
Z Light naphtha in liquid products (up to, and including, o-xylene)	18	22	31	30	20	40	27	33	32	17	42
Major constituents (% wt of liquid products)											
Cyclopentane	0.10	0.15	0.30	0.40	0.20	0.52	0.24	0.30	0.29	0.32	0.33
n-Hexane	0.40	0.82	0.70	0.75	0.54	1.08	0.64	0.87	0.77	0.21	0.90
Methylcyclopentane	0.76	0.72	1.33	1.78	1.13	1.88	0.55	0.78	0.70	0.18	0.68
Benzene	0.23	0.77	1.03	1.57	1.02	1.60	0.01	0.70	0.22	1.08	<0.01
Cyclohexane	0.78	1.03	1.94	1.06	1.24	2.30	3.44	2.72	3.67	0.07	6.41
n-Heptane	0.42	0.81	0.82	0.72	0.69	1.03	0.73	1.17	0.89	0.63	1.09
Methylcyclohexane	1.59	0.72	3.75	2.33	2.67	4.62	8.00	6.53	8.32	0.29	13.24
Ethylcyclopentane	0.17	0.52	1.34	0.99	1.01	1.44	0.38	0.44	0.38	0.24	0.38
Toluene	1.61	3.18	4.19	5.14	4.41	5.45	0.18	3.47	1.41	4.33	0.13
n-Octane	0.45	0.64	0.68	0.57	0.58	0.80	0.59	0.99	0.72	0.82	0.90
Ethylcyclohexane + ethylbenzene	1.60	1.86	2.26	2.08	2.82	2.76	2.65	2.79	3.12	1.33	3.59
Xylenes	2.45	3.03	4.15	4.51	4.48	4.10	0.10	3.41	1.70	4.07	0.28
Benzene/cyclohexane	0.29	0.75	0.53	1.48	0.82	0.70	<0.01	0.26	0.06	~15	<0.01
Toluene/methylcyclohexane	1.01	4.42	1.12	2.21	1.65	1.18	0.02	0.53	0.17	~15	0.01

KEY S = beforehand
P = in-situ
O = not pre-sulphided

TABLE 6 Carbon and sulphur contents of recovered catalysts

Hydrotreating T°C	400										300	
	HTO					HTO					HTO	
Catalyst type	Ni	Mo	Ni/Mo	Co/Mo	Ni/Co/Mo	Alumina	Ni/Mo	Ni/Co/Mo	Pd	O	Ni/Co/Mo	Pd
Active metals	S	S	S	S	S	P	P	P	O	O	P	O
Pre-sulphiding												
% C	3.9	2.6	4.6 (2.2)	3.6 (2.9)	3.6	3.3	4.4 (1.5)	8.1 (5.0)	2.6		8.1 (5.0)	6.2 (3.5)
Δ % C (+)	3.3	1.3	3.4 (1.2)	1.9 (1.3)	2.0	1.9	4.4 (1.5)	4.7 (1.6)	ND		4.7 (1.6)	ND
% S	2.3	3.0	5.1	4.9	4.9	ND	ND	ND	ND		ND	0.3
Δ % S (-)	1.6	0.2	0.3	1.3	1.3	ND	ND	ND	ND		ND	ND

Deactivation experiments

Pass No.	1	2	3	4	5	6
Ni/Mo HTO catalyst % C	4.2	4.9	5.5	5.8	7.2	8.2
Δ % C	2.5	3.2	3.8	4.1	5.5	6.5
Ni/Mo on alumina % C ^a	6.3	8.3	7.7	7.7	9.0	11.6

KEY S = beforehand () = after extraction with dichloromethane
P = in-situ ND = not determined
O = not pre-sulphided a = Δ % C since initial catalyst contains no carbon

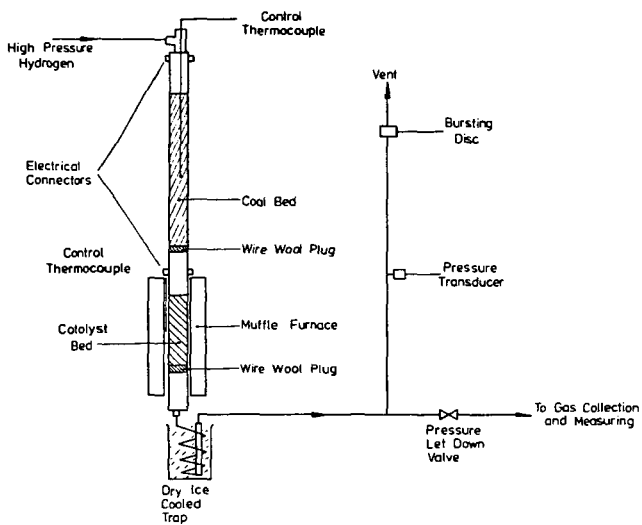


FIGURE 1. SCHEMATIC OF FIXED-BED TWO-STAGE HYDROPYROLYSIS REACTOR

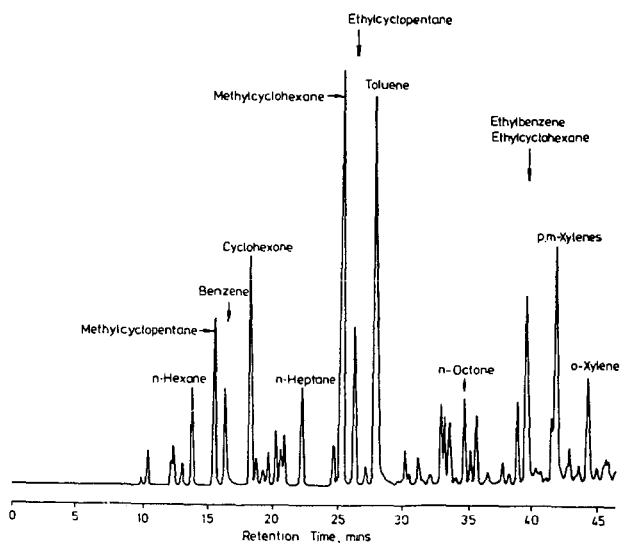


FIGURE 2 GAS CHROMATOGRAM OF LIGHT NAPHTHA FRACTION FROM THE PRODUCT OBTAINED WITH THE Ni/Mo HTO CATALYST

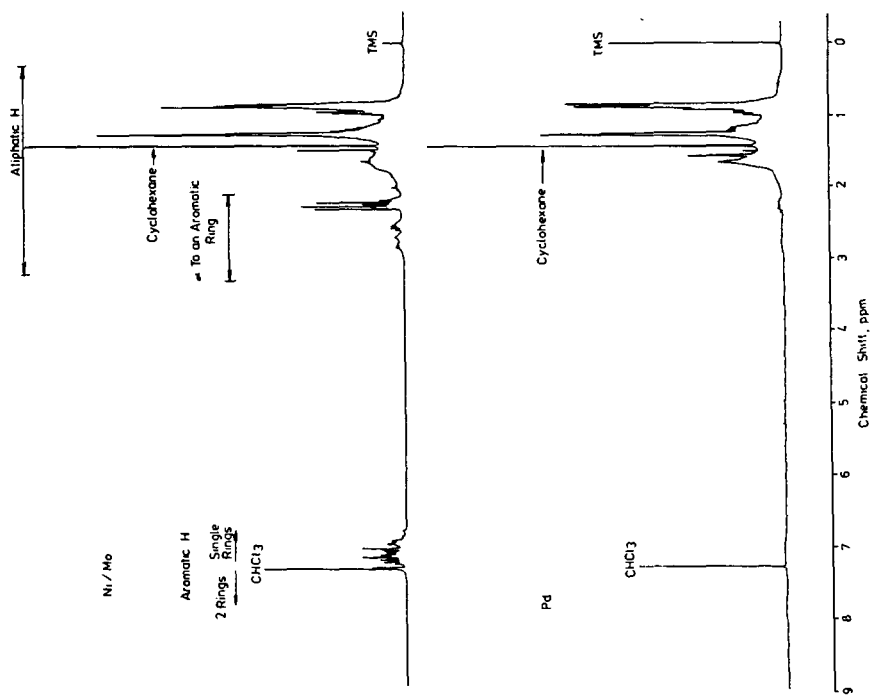


FIGURE 3. ¹H NMR SPECTRA OF LIQUID PRODUCTS OBTAINED WITH HTO CATALYSTS

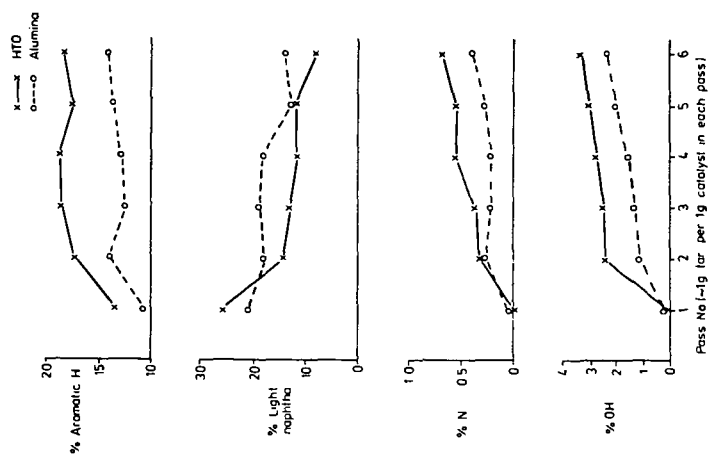


FIGURE 4. EFFECT OF DEACTIVATION ON PRODUCT COMPOSITION FOR THE Ni/Mo CATALYSTS

Role of Iron Vacancies in Pyrrhotite-Catalyzed Liquefaction
Using H_2S and CO

J. Nowok and Virgil I. Stenberg

Department of Chemistry, University of North Dakota,
Grand Forks, North Dakota 58202

INTRODUCTION

As a part of continuing investigations into the chemistry of liquefaction catalyzed by metal sulfides, a study was made of the interaction of H_2S and CO with the pyrrhotite surface using ESR spectroscopy. Minerals contained in coals are reported to promote hydrogenation and hydrodesulfurization in low-rank coal conversion processes (1,2). More specifically, those containing iron are found to promote both hydrogenation and desulfurization reactions (3). In the pyrite and pyrrhotite forms, iron has hydrogenation activity (4-6). The liquefaction activities of iron sulfides in the absence of added H_2S are distinguished by sulfur concentration and shown to be $FeS_2 > Fe_2S_3 > Fe_{1-x}S > FeS$ (7). However, pyrite quickly decomposes to pyrrhotite at liquefaction temperatures (8,9). Consequently, the catalytic activity of iron sulfides is attributed to a combination of pyrrhotite and H_2S (10,11).

Transition metal-catalyzed hydrodesulfurization has been related to the ability of these to form and regenerate sulfur vacancies (12). The catalyst is also sensitive to the number of metal vacancies (6). The variability of the composition of iron sulfides, $Fe_{1-x}S$, found in liquefaction residues is consistent with these conclusions.

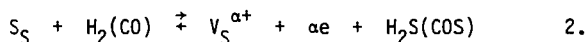
FeS is of the NiAs crystal-type and is a d^6 high-spin quintet state solid with metal properties. In an octahedral field, the d orbitals are split into two energy levels, t_{2g}^3 and e_g^3 (13). The non-stoichiometric crystal-related form of triolite (FeS) is pyrrhotite. The latter includes a wide group of iron sulfides, $Fe_{1-x}S$ with $0 < x < 0.2$ (14). All form superstructures with ordered iron vacancies and ordered spins (15). The pyrrhotites are formed by either pyrite decomposition with subsequent crystal transformation or sulfur incorporation to FeS lattice by reaction with sulfur or H_2S , cf. reaction 1

(16). S_S , $V_{Fe}^{\alpha-}$ and h^+ represent sulfur on its normal lattice position, an α times ionized iron vacancy, and an electron hole, respectively.



V_{Fe} vacancies create electron acceptor energy levels which, in turn, induce electron transfer from the surrounding lattice sulfur ions. This electron transfer process creates electron deficient orbitals or "holes" (17). For non-stoichiometric sulfides such as, $Fe_{0.996}S$, the 3p(S) holes are present in such numbers ($\sim 10^{20}/cc$) that they form an impurity energy level which overlaps in energy with the 3d Fe(II) energy level (21). This gives rise to a large increase in density of states mainly in direction parallel to the C axis (9) and disturbs electrons distribution in t_{2g} and e_g levels.

The existence of an active catalytic site is now postulated to be localized on iron ion and its surrounding matrix. The disturbance of the 3d Fe^{2+} orbital electron distribution brought about by iron vacancies gives rise to the catalytic active centers on the solid surface. Also, there appears to be a secondary catalytic effect connected with formation and regeneration of sulfur vacancies, $V_S^{\alpha+}$ (12). The latter occur in the sulfur sublattice and are formed according to reaction 2.



EXPERIMENTAL

A. Catalyst Preparation

The pyrrhotite received from the coal cleaning operation of the U.S. Steel Robena Mines, Pennsylvania, were ground and sieved through a 200-mesh screen (75 μm). The BET surface area of the catalysts used in experiments ranges between 5 and 8 m^2/g (18).

B. Liquefaction Procedure

The Big Brown lignite (C, 74.1 wt %; H, 5.4 wt %; N, 1.3 wt %; O, 18.1 wt %; S, 1.1 wt %; Texas) used in the experiments was ground and sieved through a 200-mesh screen. The moisture content was 26.1% as received, and mineral

amount was 9.2%. Approximately 1 g of the coal sample was inserted into the 12-ml tubing reactors constructed of 316-stainless steel. The reactors were additionally charged with catalyst (about 0.15 g), with water (0.8 g) and by gases: $\text{H}_2\text{S} = 1.75$ MPa, $\text{H}_2 = 3.5$ MPa and $\text{CO} = 3.5$ MPa. The liquefaction experiments were carried out at temperatures ranging from 573-773°K for 60 min. Conversion to volatile products was calculated on moisture-ash free (MAF) coal basis after heating samples at 523°K in vacuo (~ 1 mm Hg) for 5 hrs (19).

C. ESR Measurements

ESR investigations were performed on powdered pyrrhotite in a vacuum as well as under CO , H_2S , or a CO and H_2S mixture over the range of temperature 293-773°K. The pyrrhotite was added into the ESR glass sample tube which was connected with a vacuum line and reactant gas cylinders applied. The vacuum was 10^{-1} torr and that of the gases were 0.05-0.10 MPa each. The samples were outgassing at room temperature for 0.5 hr before introducing the reactant gases. All ESR spectra were recorded using a Bruker ER-420 spectrometer employing 100-kHz modulation with a resonance frequency 9.86 GHz. A polycrystalline sample of DPPH ($g = 2.0036$) was used as a g -marker when investigations were performed at room temperature.

RESULTS

1. Catalysis of BB1 Lignite Hydroliquefaction by Iron Sulfide Catalysts

In a previous article (19), the conversion of BB1 into volatile products in the $\text{H}_2\text{S}-\text{H}_2\text{O}-\text{H}_2-\text{CO}$ system with no added catalyst was reported to be temperature dependent. Using the same experimental conditions, pyrrhotite was shown to increase the conversion into distillate of BB1 lignite over the temperature range of 573-773°K with constant 60-minute time (Figure 1) and the time range of 0-60 minutes with constant 420°C reactor temperature (Figure 2). The latter conversion results followed the equation, $\text{conversion} = k \cdot t$ where k is conversion coefficient and t is time. Pyrrhotite is more active with $\text{CO}-\text{H}_2\text{S}-\text{H}_2\text{O}$ than with $\text{H}_2-\text{H}_2\text{S}-\text{H}_2\text{O}$ (Figure 3). Under the reactor conditions at 693°K for 1 hr but in the absence of coal, the conversion of CO into CO_2 with added H_2S was equal to 5.3%. Using pyrrhotite at the same experimental conditions, it was 6-fold greater (31.7%).

2. Electron Spin Resonance Spectra of Non-stoichiometric Iron Sulfides

A. Pyrrhotite-H₂S-CO System

The ESR spectrum of Fe_{1-x}S contains a broad resonance signal and a narrow resonance signal in the 3.10 g region (Figure 4). The latter is the focus of attention herein and is assigned to high spin iron(II) in its surrounding matrix (20). The spectra are recorded either in vacuum (Figure 4a), H₂S (Figure 4b), or CO (Figure 4c). The signal is split into two in vacuum at 388°K, with H₂S at 293°K, and with CO at 408°K. Both the relative intensities of the two signals (A and B) and their g-values are temperature dependent (Figure 5). Above 593-663°K, the CO-pyrrhotite signal becomes reversibly broadened. The CO-pyrrhotite ESR signal change is modified by the presence of H₂S (Figure 5). The signal changes are reversible.

DISCUSSION

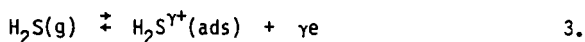
The liquefaction yields of distillate products are markedly improved in the presence of pyrrhotite as opposed to those reactions done in its absence. These data suggest that chemisorption occurs between the reacting gases and the pyrrhotite. The principal purpose of this study is to obtain direct evidence for this interaction. The ESR technique is used as the principal tool.

The sharp ESR signal of pyrrhotite in vacuum demonstrates the paramagnetic behavior of the Fe(II) ion in its solid matrix. This Fe(II) ESR signal splits into two, A and B, above 388°K (Figure 4a). The new ESR signals are now assigned to be a consequence of an electron transfer process in the solid matrix. Specifically, electrons are believed to be transferred from sulfide, S⁻², into the iron vacancy, V_{Fe}^{α-}. The reduced charged S²⁻ which is formed is electronegative, i.e., it has a hole (ah⁺). The crystal field is changed with the consequence of changes in the spin intrinsic magnetic moment of the nearest neighbor cations so the two spin couplings of the shifted orbitals are induced. An interaction between the sulfide hole and paramagnetic iron ion occurs which gives rise to peak A. The weaker interaction between the trapped electron on iron vacancy and paramagnetic iron ion moment gives rise to peak B.

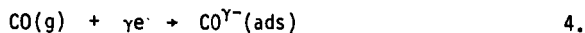
The changing g-values of ESR peaks A and B with four conditions as the temperature is increased are shown in Figure 5. The g-value variation of peaks

A and B with temperature indicate changes in the crystal electric field. These values are dependent upon the electron transfer between the adsorbate and the adsorbent.

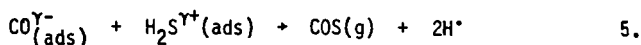
Upon exposure of pyrrhotite to H_2S at room temperature, the Fe^{2+} ESR signal is split into two separate ones (Figure 4b). Peak B resides at larger g-values (Figure 4b). This gives direct evidence for chemisorption of the H_2S onto the surface. Since the dominant chemical feature of H_2S is the electron rich sulfur and the H_2S^+ molecular cation was recently reported (22), the chemisorption process is interpreted as the occurrence of charge transfer from the electron rich H_2S onto the pyrrhotite surface (reaction 3). The free electrons formed by this means are delocalized into the iron vacancy band probably throughout 3d Fe^{2+} band.



CO, in contrast to H_2S , is ordinarily an electron acceptor in charge transfer processes. At room temperature, its presence does not alter the sharp ESR signal of pyrrhotite. However, the signal is significantly split and altered with increasing the temperature (Figure 5). This g-value variation is assigned to CO^- species formed after electron transfer from iron vacancy band, reaction 4 (23-25). The intensity of peak A is more altered than peak B by the presence of CO.



The summary significance of the reactions 3 and 4 is that hydrogen sulfide and carbon monoxide are both activated by the pyrrhotite surface to chemically react according to equation 5. When CO and H_2S are together in the presence of pyrrhotite, peak A is little altered with temperature. This is consistent with reactions 3 and 4 simultaneously occurring on the pyrrhotite surface resulting in the production of COS (reaction 5). The active hydrogen, H_1 , is consumed by the liquefaction media.



Under high H_2S partial pressures in the reactor, the Mössbauer Spectrum (18) showed the presence of FeS_2 . FeS_2 is much reduced if not absent when the partial pressure of H_2S is reduced. Therefore, the production of COS by $CO + H_2S$ occurs together with the transformation of $Fe_{1-x}S$ into FeS_2 .

ACKNOWLEDGEMENT

We are grateful for the financial support of the United State Department of Energy.

REFERENCES

1. J.A. Guin, A.R. Tarrer, J.M. Lee, L. Lo and Ch.W. Curtis, *Ind. Eng. Chem. Process Des. Dev.* **18**, 371 (1979).
2. J.A. Guin, A.R. Tarrer, J.W. Prather, D.R. Johnson and J.M. Lee, *Ind. Eng. Chem. Process Des. Dev.* **17**, 118 (1978).
3. A. Attar, *Fuel* **57**, 201 (1978).
4. R.M. Baldwin and S. Vinciguerra, *Fuel* **62**, 498 (1983).
5. D. Garg and E.N. Givens, *Ind. Eng. Chem. Process Des. Dev.* **21**, 113 (1982).
6. P.A. Montano and B. Granoff, *Fuel* **59**, 214 (1980).
7. S. Yokoyama, H. Narita, T. Yoshida, R. Yoshida, Y. Hasegawa and Y. Maekawa, *Symp. on Chem. Coal Liquef. and Catalysis*, Hokkaido Univ., March 17-20, 1985, Sapporo 060, Japan, p. 155.
8. A.S. Bommannavar and P.A. Montano, *Fuel* **61**, 523 (1982).
9. P.J. Cleyle, W.F. Caley, I. Stewart and S.G. Whiteway, *Fuel* **63**, 1579 (1984).
10. P.A. Montano and V.I. Stenberg, *Proceedings, 1985 National International Conference on Coal Science*, Sidney, Australia, 788-791.
11. V.I. Stenberg, T. Ogawa, W.G. Wilson and D. Miller, *Fuel* **62**, 1487 (1983).
12. T.A. Pecorano and R.R. Chianelli, *J. Catal.* **67**, 430 (1981).
13. T.A. Bither, R.J. Bouchard, W.H. Cloud, P.C. Donohue and W.J. Siemons, *Inorg. Chem.* **7**, 2208 (1981).
14. D.J. Vaughan and J.R. Craig, *Mineral Chemistry of Metal Sulfides*, Cambridge Univ. Press, Cambridge, 1978, p. 12.
15. E.F. Bertaut, *Acta Cryst.* **6**, 557 (1953).
16. F.A. Kroger, *The Chemistry of Imperfect Crystals*, North-Holland, Amsterdam, 1964.
17. L.A. Marusak and L.L. Tongson, *J. Appl. Phys.* **50**, 4350 (1979).
18. P.A. Montano, V.I. Stenberg and P. Sweeny, *J. Phys. Chem.* **90**, 156 (1986).
19. V.I. Stenberg and J. Nowok, *Fuel* accepted for publication.
20. W. Low and E.L. Offenbacher, *Solid State Physics* (ed by F. Seitz and D. Turnbull) **17**, 135 (1965).
21. S.L. FinkTea III, Cathey LeConte and E.L. Amma, *Acta Cryst.* **A32**, 529 (1976).
22. Ibuki Toshio, *J. Chem. Phys.* **81**, 2915 (1984).
23. P.C. Stair, *J. Am. Chem. Soc.* **104**, 404 (1982).
24. R.J. Madrix and J. Benziger, *Ann. Rev. Phys. Chem.* **23**, 285 (1978).
25. L.H. Dubois and B.R. Zegarski, *Chem. Phys. Lett.* **120**, 537 (1985).

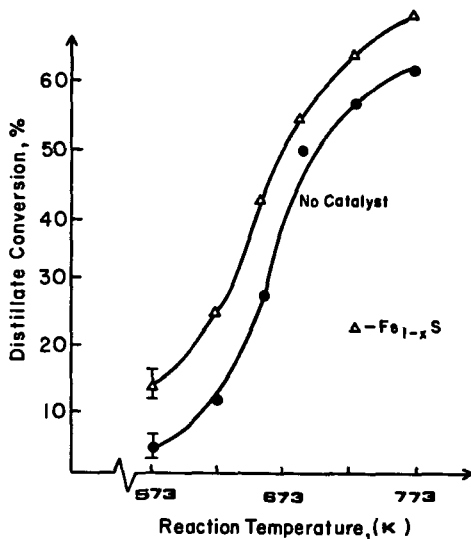


Figure 1. The effect of temperature on catalytic liquefaction of BBI lignite in $\text{H}_2\text{S-H}_2\text{-CO-H}_2\text{O}$ system. The time of the reaction was 1 hr. The pressures of the gases were: H_2S , 1.75 MPa; H_2 , 3.5 MPa; and CO , 3.5 MPa. Water (0.8 g) was added.

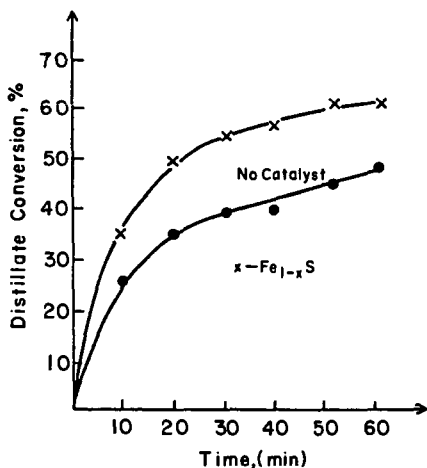


Figure 2. Kinetics of BBI lignite liquefaction at 693 K with and without catalyst in $\text{H}_2\text{S-H}_2\text{-CO-H}_2\text{O}$ system. The temperature of the reaction was 420°C, and the rest of the contents were those given for Figure 1.

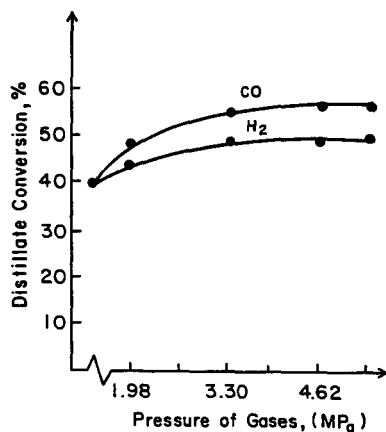


Figure 3. The effect of H_2 - H_2S - H_2O and CO - H_2S - H_2O on conversion yields. The liquefaction reactions were performed at 693 K for 1 hr with water = 0.8 g and $H_2S = 1.75$ MPa.

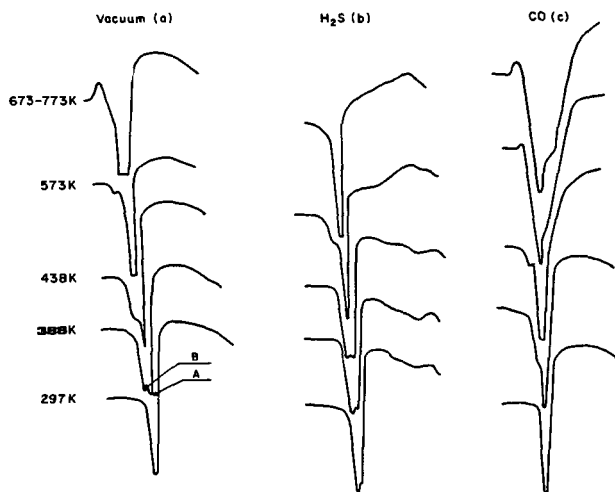


Figure 4. ESR signal of high spin iron (II) with $g = 3.10$ detected in vacuum (a), H_2S (b) and CO (c) at the range of temperatures 293-773 K.

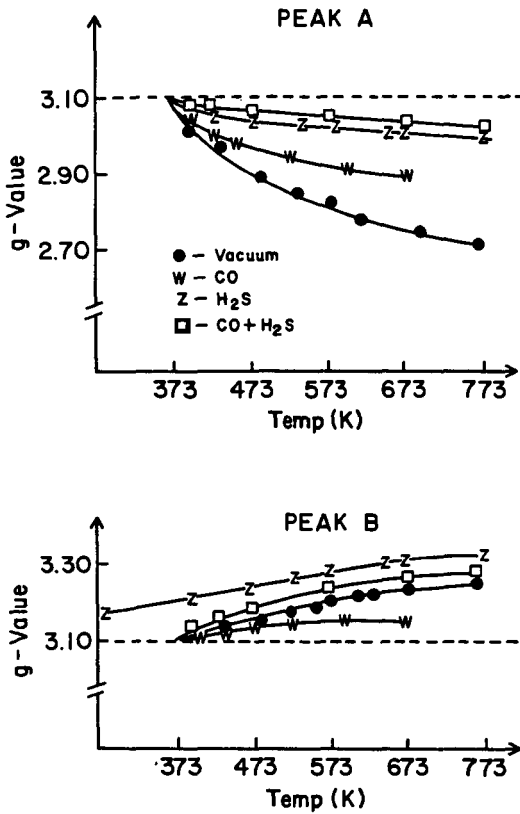


Figure 5. The variation of g-values of splitting Fe^{2+} signal detected in vacuum, H_2S , CO and $H_2S + CO$ gases.

EFFECT OF TEMPERATURE PROGRAMMING ON THE LIQUEFACTION
OF INDIANHEAD LIGNITE IN AN INORGANIC (H₂S-H₂O) SOLVENT SYSTEM

P.G. Sweeny, V. Gutenkunst, M.E. Martin-Schwan and V.I. Stenberg

Department of Chemistry, The University of North Dakota
Grand Forks, North Dakota 58202

ABSTRACT

High conversions can now be achieved using lower reactor temperatures and a temperature programming technique. Various temperature programs using times between 7.5 and 60 minutes and temperatures from 300° to 480°C were used to liquefy Indianhead lignite. The inorganic solvent system H₂S-H₂O was used in conjunction with CO, H₂ and pyrrhotite as the liquefaction media. Programming the temperature produced higher THF soluble and cyclohexane soluble yields than the use of isothermal temperatures. The maximum overall conversions obtained to date using temperature programming were 94.8% THF solubles, 83.2% toluene solubles and 70.5% cyclohexane solubles. THF-soluble conversions over 90%, were obtained at 350°C with temperature programming.

INTRODUCTION

Most modern coal liquefaction processes consist of heating a coal in the presence of a hydrogen donor solvent and an overpressure of reducing gas. The theory behind such procedures is that coal molecules are homolytically cleaved at the elevated temperature (equation 1) and then hydrogenated by either the solvent (equation 2) or the reducing gases (equation 4) (1-4). Complicating this scenario is the possibility that thermally generated coal radicals dimerize to produce high molecular weight products (equation 5). The occurrence of radical-radical reactions and their deleterious effect on coal liquefaction yields have been reported (5).



When the above mechanism operates during coal liquefaction, maximum liquid yields will be produced when the rate of coal-derived radical formation does not exceed the rate of hydrogen atom donation. If coal radicals are generated rapidly by a sudden thermal jump, then the capability of the solvent/gas system to donate hydrogen atoms by equations 2 and 3 might not be able to compete effectively with the dimerization step (equation 5). The goal of this investigation was to use various temperature programs to match the rate of radical production with the solvent/gas system's ability to cap these radicals and determine if such a procedure could substantially increase liquefaction

yields. Initial reports on the use of temperature programming have been favorable (6,7).

EXPERIMENTAL

A 12-ml batch autoclave (8) was used for the present study. For all reactions, 1 g of as mined Indianhead (Zap, ND) lignite ground to > 200 mesh was charged along with 1 g H₂O, 0.117 g pyrrhotite, Fe₇S₈, ground to > 200 mesh, 250 psi H₂S, 490 psi CO₂ and 490 psi H₂ into the autoclave. The heating block was preheated to the initial temperature, and the autoclave reached the initial temperature 2.0 min after insertion. After reaction, the products were washed with the desired solvent into a glass fiber soxhlet extraction thimble and extracted until constant weight was achieved. The proximate and ultimate analyses of Indianhead lignite are: moisture 29.5%, ash 9.0% moisture free (mf), carbon 65.0% mf, hydrogen 4.2% mf, nitrogen 1.9% mf, sulfur 0.8% mf and O₂ 19.1% mf by difference.

RESULTS

The results obtained from employing various temperature programs to liquefy Indianhead (Zap, ND) lignite are shown in Tables 1 and 2. The temperature programs used are portrayed in Figure 1. Use of Figure 1 in conjunction with Tables 1 and 2 will simplify the correlation of the temperature programs to conversion levels.

Simply increasing the residence time of lignite in the autoclave at 300°C (Figure 1, +A+B+C+D) initially enhanced the conversion to tetrahydrofuran (THF), toluene and cyclohexane solubles (Table 1). When the reaction was continued for longer times, e.g., 60 minutes, the THF-soluble products decreased in amount from that of shorter reaction times at that temperature.

Increasing the temperature from 300°C to 350°C (Figure 1, +E+F+G+H) enhanced the conversion to THF, toluene and cyclohexane solubles. Leaving the autoclave at 350°C for times up to 37.5 minutes (Figure 1, point G) produced increased yields of all three categorized products. Once this time was reached, no further increases in product yields were obtained by extending the residence times; in fact, a slight decrease in THF solubles was noted.

Employing a final reaction temperature of 400°C (Figure 1, +I+J+K+L) yielded higher levels of conversion products than 300° or 350°C. Increasing the residence time at this temperature to a total time of 20.0 min (Figure 1, point J) increased all product yields. Further increases in the residence time had little effect on the THF-soluble product yield while the toluene solubles increased then decreased with residence time and the cyclohexane solubles increased slowly.

When 450°C was the final reaction temperature (Figure 1, +M+N+O) prolonged residence times increased the toluene soluble products but had no effect on the THF and cyclohexane-soluble yields. Increasing the temperature to 480°C (Figure 1, +P) enhanced the cyclohexane solubles but did not increase THF-soluble yields.

The use of temperature programming (varied heating rates up to a maximum temperature) enhanced liquefaction yields over isothermal employment of this maximum temperature (Table 2). The THF- and cyclohexane-soluble yields at 450°C are both much greater in the programmed runs than in the isothermal ones.

Results obtained from temperature programs at which an initial heating period at 300°C was employed are shown in Table 3 and Figure 2. The conversions to THF solubles so obtained were larger than the those already

described. This demonstrates that the heating rate of the initially chosen program was too fast to produce maximum conversions. The toluene and cyclohexane solubles were also generally but not uniformly higher when the second program was used instead of the first.

DISCUSSION

The results of the temperature programmed runs demonstrate that the rate at which a liquefaction system is heated can dramatically vary the extent of conversion observed. The temperature program to 480°C produced slightly higher yields than the isothermal case. The temperature program to 450°C produced higher conversions than the isothermal use of this temperature. With temperature programming to 350°C in the more refined mode of Figure 2 (data in Table 3), THF-soluble products were produced in yields of 91.6-94.6%. These results are consistent with the hypothesis that enhanced liquefaction yields can be obtained if the coal-derived radicals are generated slowly in order to enhance the efficiency of the hydrogen donating media. Therefore, high conversion levels can be obtained through the employment of lower temperatures via the temperature programming technique.

ACKNOWLEDGEMENT

We are grateful for the financial support of the United States Department of Energy.

REFERENCES

1. Wiser, W.H. *Fuel* 47, 475 (1965).
2. Neavel, R.C. *Fuel* 55, 237 (1976).
3. Curran, C.P.; Struck, R.T.; Gorin, E. *Ind. Eng. Chem. Proc. Des. Dev.* 6, 166 (1967).
4. Gun, S.R.; Sama, J.K.; Chowdhury, P.B.; Mukherjee, D.R. *Fuel* 58, 176 (1979).
5. Petrakis, L.; Jones, G.L.; Grandy, D.W.; King, A.B. *Fuel* 62, 681 (1983).
6. Makabe, M.; Ouchi, K. *Fuel* 60, 1112 (1985).
7. Stenberg, V.I.; Hei, R.D.; Sweeny, P.G.; Nowok, J. *Prepr. Div. Fuel Chem., Am. Chem. Soc* 29(5), 63 (1984).
8. Van Buren, R.L.; Stenberg, V.I. *Chem. Ind. (London)* 14, 569 (1980).

Table 1. Effect of Temperature Programming on the Liquefaction of Indianhead Lignite in H₂O-H₂S.

Final Temp. °C	Total Time (min)	Temp. Program ^f	Conversion % ^e		
			THF	Toluene	Cyclohexane
300	7.5	A	14.8	13.8	13.0
	20.0	B	50.2	16.4	17.2
	37.5	C	50.4	14.4	19.0
	60.0	D	28.2		
350 ^a	7.5	E	33.0	17.2	20.5
	20.0	F	71.8	24.9	24.1
	37.5	G	76.9	33.6	27.8
	60.0	H	72.2	32.8	28.5
400 ^b	10.0	I	47.2	29.6	26.5
	20.0	J	79.1	48.5	35.4
	37.5	K	77.7	60.1	42.4
	60.0	L	80.8	54.6	48.9
450 ^c	22.5	M	77.1	49.7	38.1
	37.5	N	82.8	58.3	56.7
	60.0	O	84.9	81.8	56.9
480 ^d	60.0	P	82.6	-	70.4

- a. Temperature programmed by ramping from 300-350°C for 2.5 min.
- b. Temperature programmed by ramping 300-350°C for 2.5 min, 5 min @ 350°C, ramping 2.5 min to 400°C.
- c. Temperature programmed by ramping 300-350° 2.5 min, 5 min @ 350°C, ramping 2.5 min to 400°C, 5 min @ 400°C, 20 min to 450°C.
- d. Temperature programmed by ramping from 300-350°C in 2.5 min, 5 min @ 350°C, ramping 2.5 min to 400°C, 10 min @ 400°C, 2.5 min ramp to 450°, 15 min @ 450°C, 22.5 min ramp to 480°C.
- e. The % of MAF lignite soluble in stated solvent.
- f. See figure 1.

Table 2. Comparison of Isothermal and Programmed Reactions.

Final Temperature °C	Total Time (min)	Temp. Program ^d	Conversion % ^a		
			THF	Toluene	Cyclohexane
480 ^b	60	Isothermal	76.4		
480 ^b	60	P	82.6		
450 ^c	37.5	Isothermal	64.7	61.1	49.6
450 ^c	37.5	N	82.8	58.3	56.7

- a. The % of MAF lignite soluble in stated solvent.
- b. Temperature programmed by 2.5 min ramp 300-350°C, 5 min @ 350°C, 2.5 min ramp to 400°C, 10 min @ 400°C, 2.5 min ramp to 450°C, 15 min @ 450°C, 22.5 min ramp to 480°C.
- c. Temperature programmed by 2.5 min ramp to 350°C, 5 min @ 350°C, 2.5 min ramp to 400°C, 10 min @ 400°C, 2.5 min ramp to 450°C.
- d. See Figure 1.

Table 3. The Conversion of Indianhead Lignite Using Initial Heating at 300°C.

Final Temp. °C	Total Time (min)	Temp. Program ^d	Conversion % ^c		
			THF	Toluene	Cyclohexane
350	40 ^a	Q	91.6	41.3	32.2
350	80 ^a	R	94.6	51.7	39.3
400	37.5 ^b	S	93.1	44.8	34.5
400	57.5 ^b	T	94.8	83.2	56.6

- a. Temperature programmed by 17.5 min @ 300°C, 2.5 min ramp to 350°C.
- b. Temperature programmed by 17.5 min @ 300°C, 2.5 min ramp to 350°C, 15 min @ 350°C, 2.5 min ramp to 400°C.
- c. The % of MAF lignite soluble in stated solvent.
- d. See Figure 2.

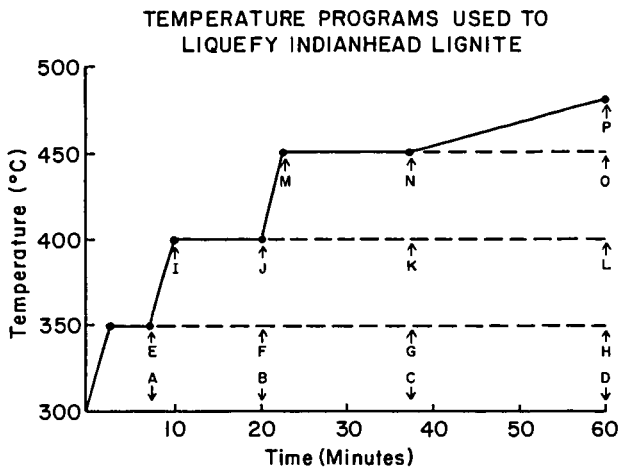


Figure 1. Temperature programs used to obtain the data in Table 1.

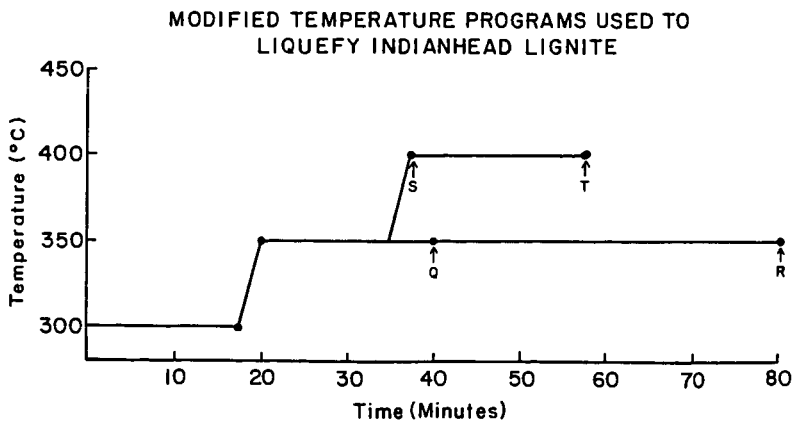


Figure 2. Temperature programs used to obtain the data in Table 3.